On the Properties of Ice at the IceCube Neutrino Telescope

A thesis submitted in partial fulfilment
of the requirements for the degree of
Master of Science

Samuel Robert Whitehead

2008

Department of Physics and Astronomy, University of Canterbury, Private Bag 4800, Christchurch, New Zealand

Abstract

The IceCube Neutrino Telescope is designed to detect high energy neutrinos with a large array of photomultiplier tubes placed deep within the Antarctic ice. The way that light propagates through the ice needs to be modelled accurately to enable the paths of charged particles to be reconstructed from the distribution of their Čerenkov radiation. Light travelling through even the purest of ice will undergo scattering and absorption processes, however the ice in which IceCube is embedded has optical properties that vary significantly with depth which need to be accurately modelled.

Currently, simulation of the muon background using the current ice model is unable to fully replicate experimental data. In this thesis we investigate a potential method of improving on the current generation of ice models. We introduce thin, highly absorbing layers into the current description of the detection medium and investigate the effect on the simulation of muon tracks in IceCube. We find that better agreement between simulation and data can be seen in the occupancy of optical modules, through the introduction of such absorptive layers into the existing ice layers.

Contents

Chapter 1

Introduction

Neutrinos are neutral, stable leptons that interact weakly with matter. Currently they are known to have a very small mass, and to come in three flavours corresponding to the three types of charged lepton. It was 26 years after its existence was predicted by Pauli that the neutrino was experimentally observed in 1956 [39]; this is a very elusive particle. This elusiveness is the very reason we wish to use it to make astronomical observations.

Since they interact via the weak interaction, neutrinos have a low probability of interacting with the many and varied constituents of the universe through which they must travel to arrive at earth. Consequently, if we can detect them then they may have originated from distant parts of our universe. Neutrino astrophysics will therefore provide us with new information about the processes occurring in the wider universe and may reveal entirely new physics, as opening new wavelength bands of the electromagnetic spectrum to observation has in the past. Unfortunately, the characteristic of neutrinos that makes them interesting to use as high energy, extra galactic messengers to observe the universe also leads to them being very difficult to detect. A very large detector volume is required to observe these particles that have such a low cross section with ordinary matter.

Although this thesis is concerned primarily with detectors located deep within the Antarctic ice, the principle of detection remains the same in detectors based deep below the ocean, or lakes. When a neutrino interacts in the detector medium, it does so by interacting with protons via the exchange of a Z or W boson, producing its charged leptonic partner. While the proton breaks into its constituent parts, creating a hadronic cascade containing many hadronic and leptonic particles, the charged lepton travels through the detector medium. Each flavour of neutrino produces a different signature in the detector but the common theme is that we detect Čerenkov radiation from the particles created in the interaction (as they pass through the medium at speeds faster than the local speed

of light).

The photons created in these interactions then make their way to the array of optical modules that make up the volume of the detector. It is very important to understand the detector medium. In order to ultimately reconstruct the path of an original incoming neutrino, we must reconstruct the paths of charged particles in the ice. These charged particles may be secondary charged particles originating from neutrino interactions or charged particles originating from cosmic rays, the latter of which we wish to reject. This path is reconstructed using the timing sequence and distribution of light detected by each of the optical modules. For this to work well, an accurate model of the optical properties of the ice medium is needed. This is the topic of this thesis. More precisely, we investigate possible improvements in the way that ice is modelled for the Antarctic based IceCube neutrino observatory. We begin, in Chapter 2, with a brief overview of neutrino astrophysics and go into more details of the detection process. It is crucial to understand the way that the optical properties of the ice are modelled, and in Chapter 3 we introduce in detail the scattering and absorption coefficients that are required to build the model. Monte Carlo simulation plays a vital role in this process, so the software used to produce results is introduced in Chapter 4. Further chapters detail current problems in simulation and investigate a possible solution. Also, we motivate potential avenues for further discussion with regard to improving the current ice description.

Chapter 2

Neutrino Astronomy

In this chapter, we motivate the construction of a large scale neutrino telescope by discussing the possibility that neutrinos can open a new observational window on our universe. High energy neutrinos are expected to be emanating from numerous sources; such sources are discussed here. We also present a short summary of activity in the field of neutrino astronomy around the world.

2.1 A New Observational Window

The Nobel prize for physics in 1978 was awarded to Penzias and Wilson of Bell labs for their rather serendipitous discovery of the Cosmic Microwave Background in 1965 [35]. This discovery came with the advent of radio astronomy and is only one of a number of discoveries that have been made upon the extension of our observations into different bands of the electromagnetic spectrum. Be it observations in visible wavelengths, radio waves, microwaves, infrared, ultra violet, X-rays or gamma rays, each part of the spectrum that we use to probe the universe reveals facts and features that broaden our knowledge and understanding.

The next window that astronomers are seeking to observe space through is that presented by neutrinos. Light has provided many exciting discoveries throughout history as we observe the cosmos. However photons, despite being unaffected by the electromagnetic fields that permeate space, are easily absorbed. Protons, which make up the bulk of cosmic rays, carry little directional information due to the influence of electromagnetic fields and at very high energies they also suffer from a tendency to interact with the Cosmic Microwave Background to produce pions, resulting in an upper limit to observed energies. Neutrinos however, are able to pass across the vast expanses of the universe relatively

unaffected. The fact that the neutrino interacts via the weak interaction means that neutrinos carry information from the very point at which they are created. By comparison, light that we see from the sun must undergo an extended "walk" from the point of its creation to the exterior surface before it is able to travel across space to reach us here on Earth, whereas neutrinos are liberated almost immediately. Neutrinos might carry all the information that they set out with, but having travelled this far with few interactions, the likelihood that they will interact in a detector on Earth is very slim.

The considerable experimental difficulty in detecting neutrinos from outside our solar system has already been overcome in one instance. Kamiokande II in Japan detected 11 neutrinos [23], IMB in the United States recorded 8 neutrino events [15] and Baksan in Russia detected 5 [8] when the supernova resulting from the explosion of the blue supergiant, Sanduleak, of the Tarantula nebula in the large Magellanic Cloud was observed in February 1987. This was proof to physicists that observing the neutrinos originating from outside our galaxy is a feasible direction in which to push new research.

2.2 Science Motivation

We seek to observe neutrinos that have travelled to us from the far reaches of space. Neutrinos that make it to Earth can be classed as low or high energy. Low energy neutrinos tend to arise from nuclear processes such as fusion in stars such as the sun while most high energy neutrinos are attributed to particle collisions in which short lived mesons decay into neutrinos - amongst other things. It is also possible that these neutrinos result from the annihilation of Weakly Interacting Massive Particles (WIMPs), a proposed form of dark matter.

It is expected that the regions of the sky that produce significant flux of high energy neutrinos will also be the areas with the most energy throughout the electromagnetic spectrum. Hadronic acceleration is the most likely process to cause both electromagnetic radiation and high energy neutrinos; Equation 2.1 illustrates how neutrinos are produced in such processes. Relativistic jets of particles are expected to produce short lived mesons, such as pions, from particle collisions. These pions will in turn decay, producing neutrinos of the energies that we are interested in detecting in neutrino telescopes worldwide.

$$\begin{aligned} p + p/\gamma &\rightarrow \pi^0 + \text{anything} \\ \pi^0 &\rightarrow 2\gamma \end{aligned}$$

$$\begin{aligned} p + p/\gamma &\rightarrow \pi^{\pm} + \text{anything} \\ \pi^{\pm} &\rightarrow \mu^+ + \nu_\mu \quad (\mu^- + \bar{\nu}_\mu) \\ \mu^{\pm} &\rightarrow e^+ + \nu_e + \bar{\nu}_\mu \quad (e^- + \bar{\nu_e} + \nu_\mu) \end{aligned} \tag{2.1}$$

There are numerous sources which could produce beams of high energy neutrinos, and IceCube's primary goal is to learn more about the processes that drive the acceleration required in current hadronic models.

- High energy neutrinos originating from transient sources. Transient sources are those which present themselves as one off bursts of energy and radiation.
  - *Gamma Ray Bursts* (GRBs) are one of the most energetic phenomena in our universe, lasting from milliseconds to minutes, yet our understanding of the processes that produce this energy is incomplete.
  - *Supernova bursts* last on the order of ten seconds, and release immense amounts of energy. Neutrinos would reach Earth before all of the light, so neutrino telescopes can provide an early warning system to observational astronomers of impending supernovae.
- High energy neutrinos originating from steady and variable sources.
  - *Active Galactic Nuclei* (AGN) emit excessive energy in many bands of the electromagnetic spectrum, indicating that they are a likely source of high energy neutrinos. AGNs are extremely bright cores of galaxies, the brightness of which is normally attributed to accretion from a super-massive black hole.
  - *Super Nova Remnants* (SNRs) are the primary distributor of heavy elements throughout the universe. The processes that allow the creation of these heavy elements within SNRs could be better understood by studying the neutrino flux radiating from them.
- *Cosmic rays* have been observed with energies as high as 3×10^{20} eV. There is currently no known mechanism that could accelerate cosmic rays up to these observed

energies. Observation of neutrino flux from neutrinos associated with cosmic ray directions would help to resolve this problem.

Aside from the exciting potential that IceCube and other neutrino telescopes have to discover these sources of high energy neutrinos, they will also be searching for neutrinos that arise from annihilation and exotic physics.

- *Weakly Interacting Massive Particles* (WIMPs) serve as one possible solution to the dark matter problem. Observations aimed at detecting the neutrinos produced by the annihilation of WIMPs that are gravitationally attracted to the centres of massive objects such as the Sun and Earth will put limits on the properties of WIMPs described in theoretical considerations.

- *Superheavy particle decay* is expected to produce neutrinos observable in neutrino telescopes such as IceCube. Many different types of superheavy particles are theoretically predicted in, for example, String, Supersymmetry and GUT models. Since the Standard Model of particle physics is not thought to be a fundamental theory, but an effective one at low energy, it is reasonable to expect that there is a theory at a new scale with associated superheavy particles. These particles, if they exist, would have been created in high numbers in the early stages of the universe's evolution. Theoretically, we should be able to see neutrinos from the annihilation of these particles. From such observation we could glean new information about particle production in the early universe.

- *Neutrino oscillations* will result in an altered ratio of neutrino flavours incident on a neutrino detector from that created at the source. The discrepancy will allow for studies of the effect of neutrino oscillations.

- *Magnetic monopoles* travelling faster than the local speed of light would emit Čerenkov radiation in the same way as a charged particle. They would however emit more Čerenkov light than a muon passing through the detector, thus producing a noticeably different signature in the detector.

Beyond this, there is the potential that stepping into the new realm of neutrino astronomy might open doors to new physics that we have yet to consider.

2.3 Neutrino Telescopes Introduced

Many experiments around the world are studying the properties of neutrinos by looking primarily at lower energy neutrinos from processes occurring in the atmosphere, the sun or other close-by phenomena. Some such experiments include Super-Kamiokande, SNO, MiniBooNE, KamLand and IMB. These detectors all enclose a volume of detecting medium within a tank surrounded by suitable shielding to reduce background interference.

The search for, and subsequent study of, sources of neutrinos outside of our solar system, primarily of high energy (the spectrum of neutrino energies is likely to extend up to energies close to 10^{20} eV), is confined to a smaller group of neutrino experiments. It is desirable to obtain directional information about incident neutrinos from the extremely low flux of high energy neutrino interactions in the Earth. In order to do this, these detectors must be of high volume, shielded from background events and of very high precision. Such a combination is gained by placing the detector below a large volume of water or ice, and by using an array of photo sensitive optical modules to detect the Čerenkov radiation emitted by the particles created when a neutrino interacts in the detector. DUMAND[1] [28], Baikal [2], NESTOR[2] [6], ANTARES[3] [1] and NEMO[4] [4,5] are all water based detectors, while AMANDA and IceCube are based under the ice of Antarctica.

DUMAND was a pioneering project and is no longer operating. Baikal is the most advanced of the water based detectors, with NESTOR, ANTARES and NEMO contributing to ongoing research toward a prospective kilometre cubed neutrino telescope to be situated in the Mediterranean Sea. Water based neutrino telescopes have a unique set of advantages and disadvantages, separate to those of ice based detectors. The main advantage is the relative ease of maintaining the array of modules. Broken or malfunctioning modules can be retrieved for repair; something which is not possible in ice. On the down side, water based detectors suffer from background light from trace radioactive isotopes and bioluminescent life forms. Deployment is also made more difficult in water, as special vessels for deploying and anchors to hold strings in place are required, along with long cables to the nearest laboratory.

[1] **D**eep **U**nderwater **M**uon **A**nd **N**eutrino **D**etector
[2] **N**eutrino **E**xtended **S**ubmarine **T**elescope with **O**ceanographic **R**esearch
[3] **A**stronomy with a **N**eutrino **T**elescope and **A**byss environmental **RES**earch
[4] **NE**utrino **M**editerranean **O**bservatory

2.3.1 AMANDA

The *Antarctic Muon And Neutrino Detector Array* is situated between 1500m and 1900m below the ice near the South Pole [10]. Ice as a detecting medium presents us with some advantages and disadvantages as compared to water based detectors. Being able to traverse the surface of the detecting medium has the obvious advantage of simplifying the deployment procedure. Holes simply need to be drilled in the ice (using a hot water drill) then the string of optical modules can be lowered to the desired height where they will freeze in place. The same property of ice allows for data to be processed and dealt with very close to the top of the strings, without the need for lengthy cables to the nearest land-based laboratory as is the case for deep sea based experiments. The primary focus of this thesis is, however, the disadvantage of dust layers within the ice. We will discuss this problem in more detail in the coming chapters, however it is useful to note that apart from the scattering and absorption from dust particles, ice is extremely transparent in the optical range of wavelengths yet free of background light (bioluminescent sea life is not a problem in the ice of Antarctica).

AMANDA has been operational since January 1997, with the upgraded AMANDA-II detector collecting data since February 2000. Since 2005 AMANDA-II has run alongside IceCube, the next generation in neutrino telescopes.

2.3.2 IceCube

IceCube is, despite the fact that it is only halfway toward completion, currently the largest neutrino telescope in the world, and will, as its name suggests, be 1km^3 in active volume, reaching down as far as 2450m below the surface of the Antarctic ice [24, 26]. Figure 2.1 shows a schematic diagram of the IceCube array. The target geometry of the detector consists of 4800 modules on 80 strings, 40 of which have so far been deployed with 18 having been deployed this summer and more planned for each Antarctic summer henceforth until the project's completion, which is expected to be in 2011. On each string there are 60 photomultiplier tubes which record Čerenkov radiation from the charged particles created when a neutrino interacts in the ice. Each photomultiplier is enclosed in a transparent pressure sphere, a Digital Optical Module (DOM). The DOM also contains a digitally controlled high voltage supply to power the photomultiplier, an analog transient waveform digitizer and LED flashers to provide test signals. The strings are lowered down a hole drilled by the Enhanced Hot Water Drill, a high velocity stream of hot water directed by gravity. Eventually the optical modules freeze in place.

The solidity of the detecting medium used in the IceCube detector allows for an additional feature that is impractical in water based detectors, namely a surface array of detectors. IceTop is a km^2 surface air shower array,installed directly above IceCube. This allows for the exclusion of downward going background from IceCube results. It consists of an array of IceTop stations each 125m apart. Each station has two 1m^2 tanks of ice spaced 10m apart, each with two optical modules.

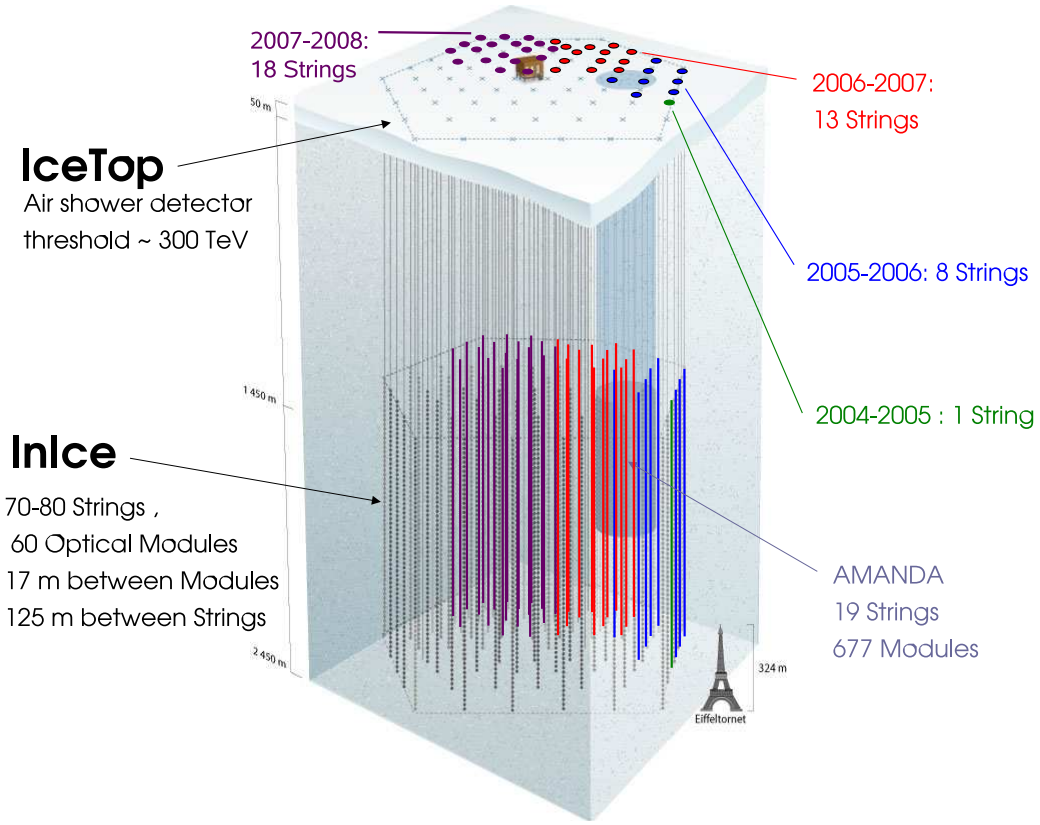

Figure 2.1: Current IceCube configuration

As of the end of the 2007-08 summer season, IceCube now has 40 strings in place. Figure from IceCube Collaboration [24].

Chapter 3

Physics of Detection

In this chapter we discuss the interactions that lead to a signal in the detector from each of the three neutrino flavours. Čerenkov photons are emitted by the charged particles created in these interactions, which then propagate through the detecting medium to the optical modules of the detector. It is thus important to understand the optical properties of the ice in order to accurately reconstruct the paths of the charged particles and, in turn, the original neutrinos.

3.1 Neutrino Interactions

Within the framework of the Standard Model of particle physics, neutrinos interact by the exchange of a W or Z boson. We are concerned with the interactions that neutrinos have with nucleons in the ice via the charged current (CC) reaction in the case of a $W^{\pm}$ boson and neutral current (NC) reaction in the case of a Z boson:

$$\begin{aligned} \nu_l + N &\rightarrow l + X \quad (CC) \\ \nu_l + N &\rightarrow \nu_l + X \quad (NC) \end{aligned} \tag{3.1}$$

with lepton flavour $l = e, \mu, \tau$, N the nucleon involved and X corresponds to a hadronic cascade.

From each of the possible reactions, a hadronic cascade always results when the nucleon is fragmented into hadrons. The subsequent interaction of these hadrons produces a further generation of particles, causing a cascade of hadronic and electromagnetic particles. The light from the cascade spreads out in a roughly spherical manner, although

it is not as bright nor as symmetric as a purely electromagnetic cascade. Currently however, the light signatures of the two cascade types are almost indistinguishable inside the detector.

The interactions that occur in 3.1, lead to different possible signatures in the detector, depending on the flavour of the incident neutrino. The charged lepton is emitted in a direction very similar to that of the incident neutrino [36].

Electron Neutrino Interaction

Through a charged current reaction, an electron is produced. The electron will then initiate an electromagnetic cascade. From bremsstrahlung, photons will be produced which, via pair production, will produce further electrons and positrons. This process extends only a small distance as compared to the spacing of the optical modules (a 100TeV electromagnetic cascade will be approximately 8.5m long [22, 38]) A cascade of relatively low energy therefore appears as a point source in the detector.

Muon Neutrino Interaction

The muon produced in a CC reaction can travel large distances (a 1TeV muon will travel up to 3km in ice). The muon is higher in mass than the electron, so undergoes less scattering, and emits fewer bremsstrahlung photons. It therefore appears as a track in the detector, so a muon neutrino event occurring outside of the detector volume can, in principle, be detected by IceCube.

Tau Neutrino Interaction

The tau lepton is a shortlived particle, which decays quite quickly, producing a second hadronic cascade. If the primary tau neutrino imparts a high enough energy onto the created tau, the hadronic cascade from the original reaction with the nucleus will be distinct from the secondary cascade caused by the decaying tau. This type of event is known as a *double bang* event, where the two cascades are joined by a short Čerenkov track. Tau neutrino events of lower energy are however indiscernible from electron neutrino events.

3.2 Background Events

When a charged cosmic ray collides with the atmosphere of the earth it can produce pions or kaons. These particles in turn will either collide with further air nuclei or decay to produce atmospheric muons and neutrinos. It is these muons, the rate of which is about 6 orders of magnitude greater than the atmospheric neutrino rate, that make up the bulk of the activity in the detector. The main shield used to remove background is the Earth; neutrinos that we focus on are those that have travelled through the earth before interacting in or near the detector. This way, all background muons that remain to be removed are coming from the opposite direction to the muons that we expect to see originating from neutrino interactions. It is important that we simulate these downgoing muons correctly, as their mis-simulation can cause problems - as will be discussed in Chapter 5.

3.3 Čerenkov Radiation

Although the speed of light in a vacuum is constant, the speed of light through a denser medium, is reduced to $c_n = \frac{c}{n}$ where c is the speed of light in a vacuum, and n is the index of refraction of the medium [19]. For ice, in the optical wavelengths for which it is extremely transparent, the index of refraction is approximately 1.31. The speed of light in the detecting medium of IceCube is thus:

$$c_n = \frac{c}{n} = 2.288492 \times 10^8 \mathrm{ms}^{-1} \tag{3.2}$$

Charged particles moving through a dense medium with speed greater than that of light through the material ($v = \beta c > c_n$) produce Čerenkov light [19]. Čerenkov radiation is emitted with respect to the direction of the motion of the charged particle at the Čerenkov angle, θ_c, according to the relation:

$$\cos\theta_c = \frac{1}{\beta n} \tag{3.3}$$

This means that for relativistic particles moving at approximately c (i.e. $\beta \approx 1$) in ice with a refractive index of 1.31, the Čerenkov angle is $\theta_c = 40.24°$.

3.4 Ice Properties

To accurately reconstruct the paths of incoming neutrinos, we need to trace the path of the light that reaches the photomultiplier tubes from the charged particles that are

created when the neutrino interacts. Although ice is very transparent to optical photons, reconstructing the intricacies of their propagation through the ice requires an understanding of its optical properties; namely scattering and absorption. For further discussion on the determination of the optical properties of ice, and how they are determined, the reader is referred to [7, 41].

3.4.1 Scattering

In his 1908 paper [32], Gustav Mie developed an analytical solution of Maxwell's equations for the scattering of electromagnetic radiation by spherical particles. Mie Scattering is appropriate for modelling light scattering in ice, as the predominant scattering centres are submillimetre sized air bubbles and micron sized dust particles. To describe this scattering we use the physics described in [7]. Generally light is scattered multiple times before we observe it. The average cosine of the light field of photons that have undergone multiple scattering obeys a simple relationship:

$$\langle \cos\theta \rangle_n = \langle \cos\theta \rangle^n \tag{3.4}$$

That is, the average cosine after n scattering events is the average scattering angle of one event raised to the power n. Another key parameter is λ_s, the geometric scattering length - the average distance between scatters.

It is useful to wrap both of these parameters up into one, λ_e, the effective scattering length. When light propagates through a medium, the centre of the photon cloud moves along the incident direction at a decreasing pace until it stops at one λ_e. The decrease in pace is due to the photon cloud spreading out more with each scatter, so that the average of the forward going components of the velocity is reduced. On average, per step, a photon advances at an angle of $\langle \cos\theta \rangle$ a distance of λ_s between each scatter. Hence after n scatters, a photon has moved in the incident direction:

$$\lambda_e = \lambda_s \sum_{i=0}^{n} \langle \cos\theta \rangle^i \tag{3.5}$$

$$\text{or} \quad \lambda_e = \frac{\lambda_s}{1 - \langle \cos\theta \rangle} \quad \text{for large } n \tag{3.6}$$

With the AMANDA and IceCube arrays, we are unable to determine λ_s or $\langle \cos\theta \rangle$ independently as the light scatters more than once in between the optical modules where it is received, but we are able to infer them through determining λ_e. Instead of λ_e,

we normally discuss scattering in terms of the effective scattering coefficient $b_e = \frac{1}{\lambda_e}$. Figure 3.1 shows the variation of the scattering coefficient, b_e, with depth.

The scattering centres for light propagation in IceCube are dust particles of various types and air bubbles.

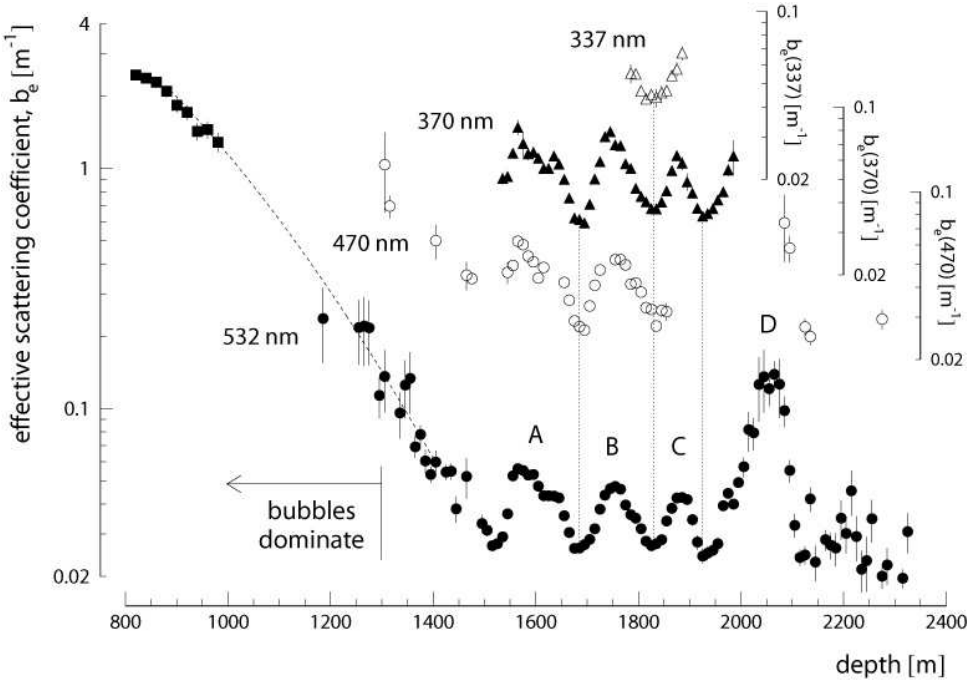

Figure 3.1: Depth dependence of scattering coefficient
The strong drop off in scattering coefficient from depths of around 1250m due to the transition of air bubble into non-scattering air hydrate crystals is clear. Below this, there are four main dust peaks present in the ice. The scattering data presented makes up the Millennium model, to be discussed in Section 3.4.3. Figure taken from [7].

Dust

In [7], in which the most recent treatment of the optical properties of Antarctic ice was developed, a four component dust model was used. The four components of the model are insoluble mineral grains, sea salt crystals, liquid acid drops and soot. Sea salt crystals and liquid acid drops contribute negligibly to absorption, with sea salt being the strongest scattering component. The insoluble mineral grains are the most common component, and contribute to both absorption and scattering, while soot contributes mainly to absorption. The relative abundance of each of these components was derived from ice core data in [21, 37]. These values included updated mass concentrations based on more recent ice cores from Vostok and Dome Fuji.

Air Bubbles

It is reasonable to assume that air bubbles would play a major role in scattering in the ice of Antarctica, which is laid down through a process of snowfall, hence trapping bubbles of air as it compacts. This is true down to depths of approximately 1250m below the surface. Below this level however, the pressure of the layers of ice above compact these air bubbles into air hydrate crystals, which have an index of refraction nearly identical to that of ice [40].

3.4.2 Absorption

The only parameter needed to describe the absorption of light in a medium is the absorption length, λ_a, defined as the distance at which the survival probability of a photon drops to $1/e$. As in the case of the effective scattering coefficient, we normally characterise the absorption by the absorption coefficient, or the absorptivity, $a = \frac{1}{\lambda_a}$.

One can parameterise the wavelength dependence of the absorptivity by a three component model [9]:

$$a(\lambda) = A_U e^{-B_U \lambda} + C_{dust} \lambda^{-\kappa} + A_{IR} e^{-\lambda_0/\lambda} \tag{3.7}$$

For further details on the values of the constants in 3.7, see [7]. The three different components of this equation are contributions by parts of the spectrum of wavelengths; the ultra-violet, visible and infrared ranges.

- The *Urbach tail* in ice extends until $\sim$ 200nm in wavelength. It is characterised by a steep exponential decrease in absorptivity at wavelengths corresponding to an electron band gap energy.

- Antarctic ice is very pure and thus in the wavelengths between $\sim$ 200 and $\sim$ 500 nm is extremely transparent, with impurities, as described above, being the main contributers to absorption in this band of wavelengths. The middle term in Equation 3.7 that describes the impurity contribution arises from Mie theory and is a simple power law.

- The third term, an exponential rise in absorptivity due to molecular absorption by pure ice, occurs at wavelengths longer than $\sim$ 500nm.

3.4.3 Measurement of Ice Properties

IceCube and AMANDA have both pulsed and steady light sources located at various positions under the ice which are used to determine the optical properties of the ice. In the case of the pulsed light sources, which include lasers and LED flashers, we can measure the distribution of arrival times at a particular receiver from a source at a given position. Due to the distances involved being in most cases too short to describe the photon arrival times analytically with the random walk function, Monte Carlo (MC) simulations are carried out to model the photon propagation in the ice. MC parameters are adjusted until an agreement is met between simulation and in situ data for photon timing distributions.

Steady light sources such as the Ultraviolet and Rainbow modules in AMANDA provide a complementary result to those obtained by means of matching MC simulation to observed data as they do not depend on any assumptions of the scattering function or parameters such as $\langle \cos\theta \rangle$ [7]. A fluence analysis is carried out, comparing time integrated photon fluxes of varying receiver distances from a given source. From this information, along with the results of the pulsed light source determination of optical properties, an ice model is born. In this thesis we consider the two most recently produced IceCube ice models, the Millennium model and the AHA model.

The Millennium Model

In [7], the format for the current generation of ice models was developed and until May 2007 the Millennium, or y2k, model was the most up to date description of the Antarctic ice available. Figure 3.2 shows the depth and wavelength dependence of the absorption and effective scattering coefficients.

The y2k model uses 10 metre depth bins with each layer having, for each of 30 wavelengths from 300 to 600nm, a specified absorptivity a, effective scattering coefficient b_e, group and phase refractive indices and average $\cos\theta$ of scattering angle to be used in further simulation. The refractive indices do not change very much from layer to layer, and $\langle \cos\theta \rangle = 0.8$, despite the average scattering angle of light in ice having been measured in ice to be 0.94. This reduces the number of calculations needed in simulation using the ice model. Tests have been successfully carried out to ensure that this change makes only a negligible difference to the overall performance of the model in simulation.

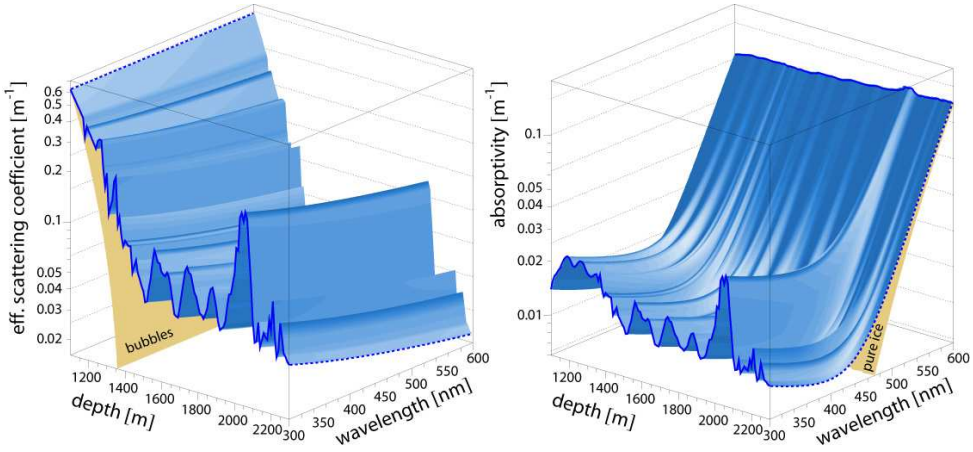

Figure 3.2: Depth and wavelength dependence of optical properties in Millennium model Figure taken from [7].

The AHA Model

During the course of this thesis work a new model of the ice at the South Pole was developed by Kurt Woschnagg and Johan Lundberg, of the IceCube collaboration, to account for known systematic problems with the y2k model. The Additionally Heterogeneous Absorption, or AHA, model was, at its conception, expected to be a far better description of the ice. To understand the difference between this and the previous model, it is important to understand why AHA was developed.

Smearing The millennium ice model is built around data obtained from in situ light sources such as flashers. To probe the optical properties of a given layer, light was inserted into the detector at one point, and measured at various optical modules in and around the same horizontal plane. If a photon originates in a layer which lies next to layers of different scattering and absorption properties than its own, then it is likely that the measured properties of that layer will be a mixture of the properties of the surrounding layers, as well as the layer in which it originates, as outlined in Figure 3.3. Each photon could spend time in the adjoining layers, therefore the measured scattering and absorption coefficients for a particular layer are actually smeared with those of adjoining layers. This effect is more prominent for larger source-detector distances, as the photon has the potential to spend more time in adjoining layers.

The AHA model sought to deconvolve this smearing effect so that when smearing occurred inside the AHA model the properties of the Millennium model would be returned. This means that the valleys and peaks in the distribution of scattering, and especially ab-

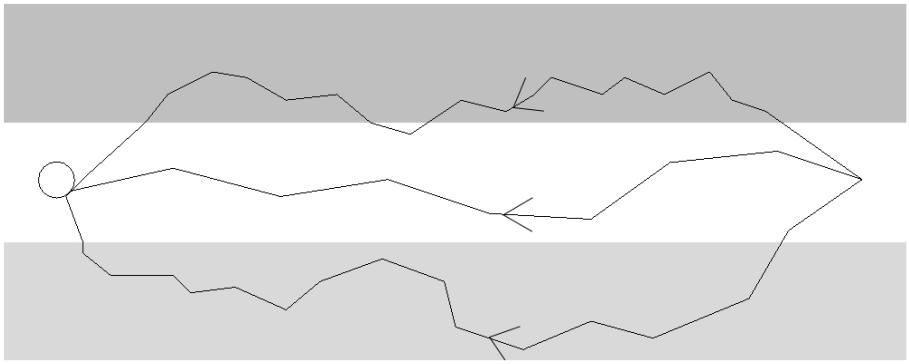

Figure 3.3: Smearing of Optical Properties
Photons emitted (right) in the same layer in which they are to be received (left) are likely to probe the surrounding layers. This smearing will result in a dirty layer appearing cleaner and vice versa. The smearing of optical properties is greater for larger source to receiver distances.

sorption, are stretched. By this mechanism, the new model should be a closer represention of the actual properties of the ice in the detector.

Deep Ice Properties The millennium model was predominantly determined through light emission and detection of the AMANDA detector as described at the beginning of Section 3.4.3. The depths below the reach of AMANDA, which are now included in the active volume of IceCube, were described in the model as being much dustier than it is now thought. Peaks in dust deposition in ice cores taken at other sites in Antarctica, in particular at East Dronning Maud Land, or EDML, can be matched to the four main dust peaks within IceCube. These same cores suggest that the ice which was laid down before these dust layers is considerably less dusty, and since IceCube is now probing these depths, it is important that our simulations represent the conditions more accurately. Consequently the properties of the deep ice is considerably cleaner in the AHA model than it was in the y2k model.

Dust Logging Technology

Current ice models were determined using in situ light sources, the best way to determine the actual absorption and scattering properties of the ice surrounding the source and receiver. With assumptions about the optical properties of particular dust types, ice cores and dust loggers offer a way to determine the vertically varying properties of the ice with more detail. When an ice core is taken at one of the sites around the Antarctic, it is possible to see the variation in contamination as a function of depth. As yet, no deep

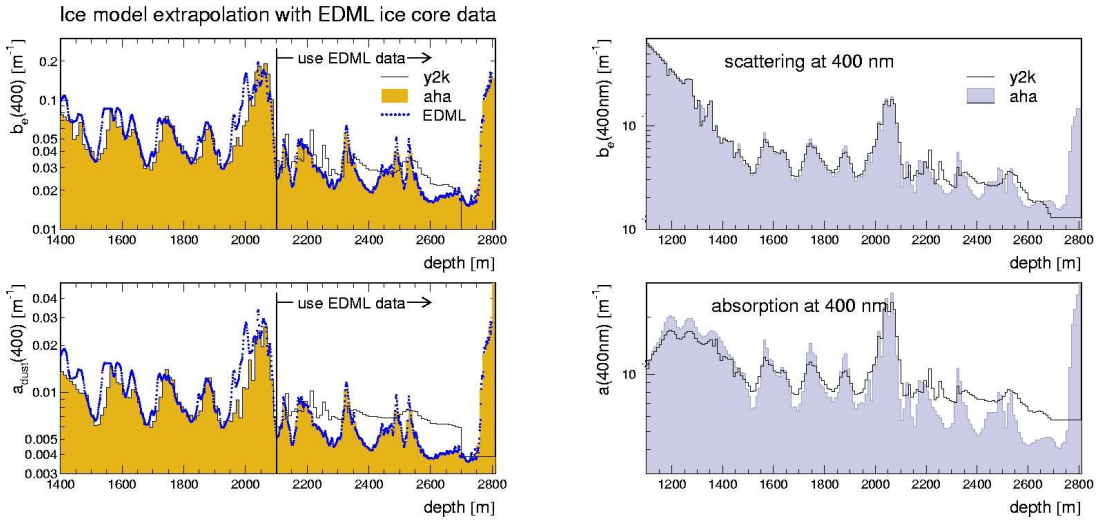

(a) Cleaned Deep Ice

(b) Comparison to y2k Model

Figure 3.4: Optical Properties of AHA Model
In plot (a), the improvement in clarity of the deep ice to follow the results of the EDML core is shown. Plot (b) shows a comparison between AHA and Millennium ice; note the stretching of the peaks and valleys in the properties. Plots produced by Kurt Woschnagg and Johan Lundberg. Figures taken from [25].

cores have been taken at the south pole, but mapping results from deep cores taken at sites such as EDML, Vostok, Siple dome and Dome C to the depths of known dusty layers at the Pole is a possibility.

Dustloggers [16, 34] offer a complementary method of registering a detailed account of the vertically varying properties of the ice. These devices are lowered into the IceCube boreholes. They consist of a light source directed horizontally into the surrounding ice vertically separated from a detector. Brushes prevent background light from passing straight down the borehole from the source to the detector. A schematic diagram of the concept is presented in Figure 3.5

As the logger moves down the borehole it records the signal received by the photomultiplier tube. Increases in signal correspond to higher concentration of scattering centres while sharp drops in signal usually correspond to peaks in absorption. In the shallower ice, bubbles provide a background of particularly high scattering which is very sensitive to dips in signal caused by absorptive layers. In the deeper ice the scattering centres are not as dense as the bubbles present at depths less than 1250m. As this process relies on measuring the amount of light returning to the detector due to the presence of scattering centres, it is not very sensitive to thin absorptive horizons, since the signal drops are not

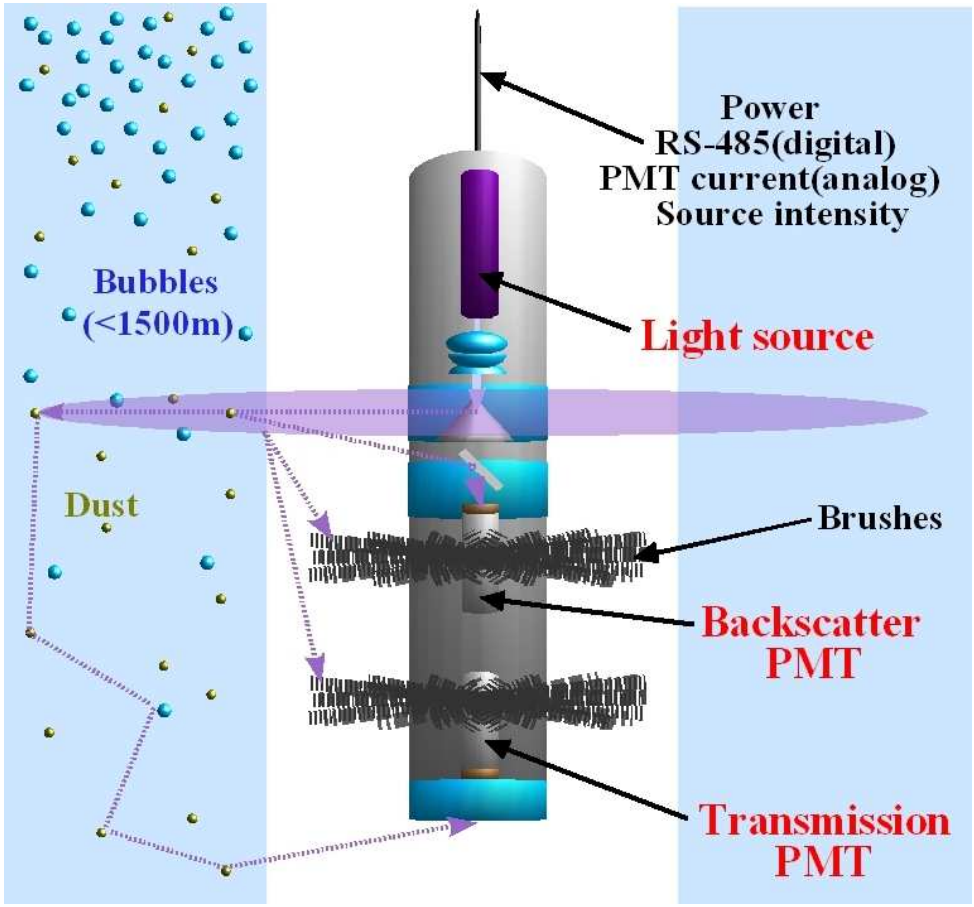

Figure 3.5: Dustlogger concept

A dust logger is an optical instrument used to measure scattering by dust in the ice surrounding a water-filled borehole. The compact device, usually 1m long, contains a collimated light source on one end, a photomultiplier tube on the other, and several brushes in between to block light reaching the PMT directly through the water. Figure taken from [25].

as well defined where there are no bubbles.

So far, four dustlogs have been made in IceCube boreholes, with further logs planned in subsequent deployment seasons. The information gleaned from these logs is useful not only in mapping the variable dust content, but also in determining whether the approximation of horizontal plane symmetry is a valid one; if corresponding dust layers are found to vary in depth, we will need to include this in future ice models. By correlating the present results obtained from dustlogs and ice cores taken at other sites around Antarctica it should be possible to determine what depths at the South Pole are likely to have more sharply varying optical parameters, leading to the possibility of a vastly improved description of the ice before the completion date of the full IceCube array.

Chapter 4

Simulation Programs

The main focus of this thesis is to attempt to improve on the current generation of ice models. To do this we need to implement software that will carry out Monte Carlo (MC) simulations of photon propagation through the ice that we model. Photonics performs this procedure, producing tables of the distribution of light as a function of distance from a given source position. The Photon Simulation Interface, working in the ROOT framework, is a tool that allows us to access and analyse the resulting photon tables. We need to simulate actual events using our ice model and then reconstruct these events to compare with IceCube data. This is done using the IceTray software.

4.1 Photonics

Photonics is a photon tracking Monte Carlo package developed by Predrag Miočinović [33], and maintained by Johan Lundberg. Photonics is a freely distributed package that calculates photon flux and time distributions in a medium surrounding a light source [29, 30]. Photonics outputs tables describing the distribution of photons for a number of different sources, which can be placed at any position in a given medium. In order to simulate the light from a moving light source (such as a relativistic muon passing through the ice) the photon flux distributions for many point-like Čerenkov emitters are integrated over.

It is important to note that the model used to describe the ice in Photonics is highly customisable. This allows changes to the accepted models to be tested with relative ease. If one wishes to add layers, or modify existing layers in pre-existing ice models, then the software can handle these changes easily. The package also comes with various tools that make the conversion from sets of point like tables to muon-like tables simple. For details of the specific MC methods that Photonics employs, see [30], a brief summary of which

is given below.

The two types of source that are usually simulated using Photonics are electromagnetic showers and Čerenkov cone emitters. Both consist of photons with wavelengths originating from a Čerenkov spectrum, however the latter are sharper emitters that are later combined to create descriptions of muon tracks.

The basic inner geometry of each Photonics table is tied to the light source symmetry axis, the direction of which is always defined as being parallel to the positive z-axis[1]. Once the geometry is defined, Photonics simulates the propagation of light from a given source through the ice. For each individual photon that is propagated, an initial weight is assigned. From its insertion, the photon propagates through the ice, its scattering being determined by an in-built scattering function that incorporates the effective scattering length and average cosine of the scattering angle of the layer in which it currently resides. These details are defined within the ice table. As the photon propagates, it can reach one of three boundaries; An ice layer boundary, a bin boundary or the center of a bin. At each of these boundaries, the weight is adjusted according to the absorption coefficient in the new region, and the scattering function is likewise adjusted. If the photon has reached the center of a recording bin, its current weight is recorded. This weight, when summed with all the other photons propagated through the medium, makes up the flux which is recorded in the Photonics table. The photon then continues through this process until its weight drops below a nominated minimum level, whereupon its passage is concluded and it is said to be absorbed. The completed Photonics table is then normalised and efficiencies applied so that the flux for a particular bin is indicative of the flux in IceCube at that point for whichever source type and orientation that the table was generated for; this is also known as a level 1 table.

4.1.1 Table Production

There are two main types of Photonics tables that one must generate in order to test a new ice model in the IceCube simulation chain. This is because we are interested in simulating detector response for primarily electromagnetic showers and muon tracks. As mentioned above, Photonics has predefined settings for several different source types, which conveniently include EM showers and Čerenkov cone emitters.

[1]Appendix A contains in depth details of the binning and scaling of the individual variables in each of these tables.

Electromagnetic Shower Tables

The first step of the production of a full set of Photonics tables is to simply create separate tables to describe the source when it occurs in any number of positions and orientations throughout the detector. In this thesis our work employs the same source spacing as established in the AHA model; 20 metre depth separation and 10 degree source axis angle separation. Since we wish to have sources that can be seen within the sensitive volume of the detector, we create sources over a range of -800m to 800m in IceCube coordinates; this corresponds to depths of approximately 1150m to 2750m, easily incorporating the detector volume. In total, we have just over 1500 tables for EM showers once this step of table production is complete.

Muon Tables

A set of Čerenkov cone emitter tables must be generated in order to describe the light from muons, which produce long tracks in the ice. Photonics currently only has the capability to produce point source tables. Adding functionality for extended line sources would not be the most optimal use of computational resources. Each source is now a simple Čerenkov cone emitter; Photonics integrates over a number of these point source tables in order to generate the muon track.

A slightly different geometry is used for these muon tables, known as level 2 Photonics tables, in which a cylinder surrounding the muon track, which may be a starting track, stopping track or degenerate (infinite) muon, is binned according to user input[2]. For a single cell of the muon geometry the program loops over the length of the muon track in question, taking the normalised flux at the desired cell from each of the level 1 tables corresponding to Čerenkov sources along the track. It then adds up all of these contributions to arrive at the flux for the cell.

4.1.2 Computing Facilities

Considering the number of calculations required to complete the generation of a full set of Photonics tables, it is essential to perform the computations on a system capable of carrying out the task in a relatively short time. The University of Canterbury's Super Computing facility was used in the latter stages of this thesis to speed up the table generation - this provided us with an increase in computing power. Since the Photonics

[2]See Appendix A for level2 binning details.

software employs an inherently serial process to arrive at the final photon tables, the only advantage of using such a system was to be able to run a greater number of jobs at any given time.

The use of the Power-PC system employed by the high performance computing facilities at Canterbury University resulted in additional problems. Since the system on which we were creating the photon tables writes to memory using the big-endian format, and the normal PCs, onto which we needed to shift the tables in order to perform the analysis, writes using little-endian format, a small adjustment of the source code of the Photonics software was required. Once implemented however, we found that Photonics ran easily on such systems.

4.2 Photon Simulation Interface

Thomas Burgess' Photon Simulation Interface, PSI, is intended as a layer between the Photonics tables and the simulation of hits in optical modules [18]. Sitting in either the IceCube software chain, or standing alone within the ROOT framework, PSI allows users to load a set of tables, specify the location of a track and the receiving optical module, and to retrieve information relating to three main quantities:

- The *Mean amplitude*, that is the number of photoelectrons produced in the photomultiplier tube.
- The *Hit time delay*, that is the difference in time that the propagating photons experience due to scattering as compared to the time taken for a photon to travel directly to the receiver.
- The *Hit probability*, that is the probability of a hit given a certain time delay.

4.3 ROOT

ROOT is an object oriented programming environment developed at CERN and although originally developed as a histogramming package in C++, it has expanded into multi-tooled framework with many features which are useful in particle physics analysis [17]. In this thesis, all histograms are produced using ROOT, but it has much more functionality than this.

4.4 IceTray

IceTray is a simulation, reconstruction and analysis framework for use in developing IceCube applications. The IceCube code is composed of discrete modular chunks that can be changed, improved, added or subtracted without affecting the others [25]. IceTray modules are independent code units which operate on a data stream. For example a module might perform a particular reconstruction algorithm, or calibrate an event. The user simply arranges the modules by writing a Python script that runs through them in such a way that the appropriate functions are being performed on the desired input stream.

4.4.1 Simulation and Reconstruction

As described in Section 3.2, the bulk of the interactions that occur in the detector are downward travelling muons. In this thesis we are primarily concerned with simulation of this background, rather than the significantly less common upward going neutrino signal. Consequently we focus on the downward travelling muons generated by high energy particles interacting in the atmosphere above the detector. The dCORSIKA[3], or *COsmic Ray SImulations for KAscade*, program provides us with an input stream for our simulation in the form of a set of showers consisting of muons varying in both energy and zenith angle. The input for the simulation is the directions and energies of these muons at the ice surface [3]. From this, we set our IceTray simulation framework up in such a way that it simulates the progress of these muons through the ice. This results in simulated hits in the detector, upon which we can perform standard reconstruction routines to see how the lit up modules would be interpreted by the detector.

[3]The d was added when the simulation software was adapted for the AMANDA detector by Dmitri Chirkin of Berkeley.

Chapter 5

Toward a More Accurate Ice Model

We currently have an ice model which, through its heterogeneous description of the vertically varying optical properties, accurately reproduces data from in situ light sources. It is however not perfect in simulation. We are able to reproduce flasher data using the current models, however problems develop when the simulation of muon tracks is performed. In this chapter we discuss these problems and motivate a potential approach to improving on the current models.

5.1 DOM Occupancy

We see discrepancies between the simulated muon background and the data from IceCube by simply observing the DOM occupancy of the simulated hits in the detector and comparing these to the real hits from a given run. The DOM occupancy is a measure of the number of hits that each DOM height receives in a given run; simulated or real. Such plots are particularly useful indicators of problems with the simulation, as the occupancy is a variable that shows depth dependence, with reduced hits in the data occurring at the same depths as known dusty layers. This reduction in hits in dusty regions of the detector is not fully taken account of in simulated data. It is particularly interesting that the AHA model, which represented a significant change to the ice model and was expected to correct such problems, is similarly poor in its likeness to the experimental results. Figure 5.1 shows the current ice models plotted against simulated CORSIKA single and coincident muons in y2k and AHA ice.

The drop-offs in occupancy occur in depths that match up very well with the known dusty layers of the ice, indicating that it is likely that the problem is associated with the description of the ice that we use.

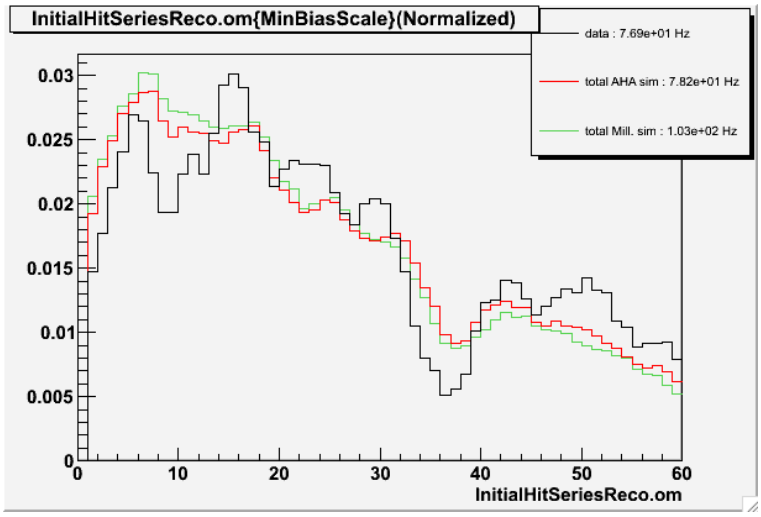

Figure 5.1: DOM Occupancy
Produced by Jon Dumm [20] from simulation of CORSIKA single and coincident muons.

5.2 The COGz Problem

When reconstructing muon tracks in the ice, an oft observed problem is the mis-reconstruction of down going muons, which make up the bulk of the background in IceCube, as up going tracks. One can visualise this as a problem with the way that the optical properties are described as in figure 5.2. Photons that travel through a particularly dusty layer of ice to reach an optical module, may take more time to do so than photons that only traverse clear areas of ice, even if the most direct path to the optical module may well be slightly further. This could result in the simulation software miscalculating the trajectory of the muon track as having passed the lower DOM first, and hence appearing as up going.

In reconstruction and analysis of events in the ice one often sees a distinct disagreement between the properties of simulated events and IceCube data. There tends to be a clustering of events centred in the clearer ice, which is not fully represented in the reconstruction of simulated background. This has been an ongoing problem throughout the AMANDA programme and has continued to appear within IceCube systems. It was previously thought that introducing a layered description of the medium would eliminate the effect, since all of the dips in the number of events correlate almost perfectly with the observed dust peaks of the accepted ice model. This however has not been the case for IceCube analyses. The variable that is most sensitive to this discrepancy between experiment and simulation is the distribution of the z-coordinate of the mean position of all hits (otherwise known as COGz). The data in which we observe the COGz problem

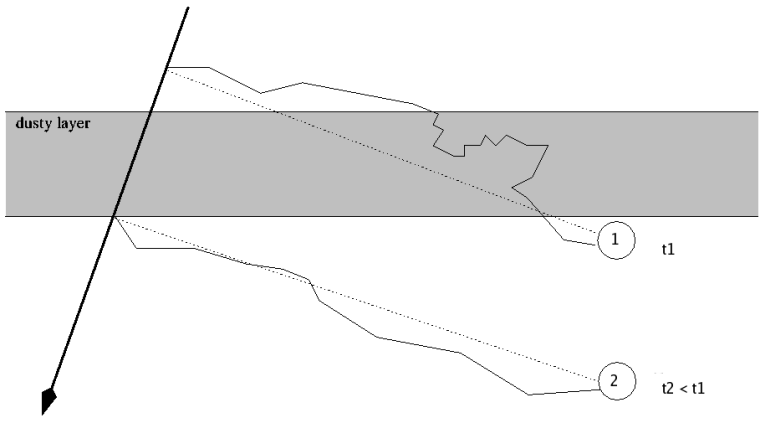

Figure 5.2: Mis-reconstructed Muon Track
As a downward travelling muon passes through a dusty layer, it is possible that photons which are emitted earlier are in fact received later due to increased scattering in such layers. This results in the earlier hit being recorded below the layer, and the muon appearing to be travelling upward.

has undergone a substantial number of cuts. Although the exact data reductions made in any specific analysis of AMANDA or IceCube data are decided upon by the author, initial filtering to pick out events of a particular type and usually some cuts on likelihood parameters and number of hits are normal. A cut is then usually made on the reconstructed muon zenith angle, to remove all muons that have been correctly reconstructed as downgoing. After this cut, it is apparent that the muon background is not being simulated correctly, as the distributions of COGz from data and simulation are quite different. In some analyses cuts are made on the COGz variable, which remove events with COGz in slices of the detector that contain unsimulated background. If the problem were corrected a larger proportion of the detector could be used in the search for extra galactic neutrino sources.

5.2.1 Ice Systematics Studies

Using 2003 AMANDA data and simulations that employ the y2k ice model Stephan Hundertmark defined a parameter called the relative OM sensitivity as the hit rate in data divided by the hit rate in simulation for a given optical module. The distribution of this sensitivity parameter showed a correlation with the known dust peaks.

This observation that the sensitivity of each module was tied to the ice model led to studies of the systematics of the ice property measurements that resulted in the y2k model being re-evaluated. As discussed in Section 3.4.3, studies of these systematics revealed a

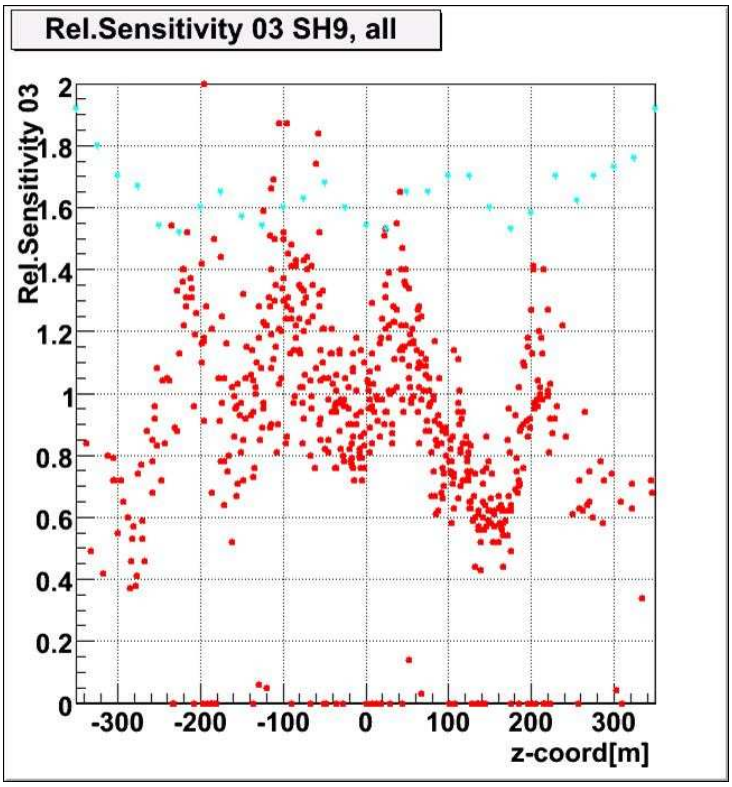

Figure 5.3: Distribution of relative OM sensitivity parameter
Stephan Hundertmark introduced a sensitivity parameter that clearly shows variation with depth, indicating a coupling with the ice properties. Distances are measured in AMANDA coordinates

certain level of smearing of the optical properties in the Millennium model. This smearing was deconvolved, leading to the current AHA model.

A more sophisticated definition of optical module sensitivity was used by Jim Braun in another study [25]. He calculated the number of expected photoelectrons for tracks near the OM by fitting the photoelectron expectation as a function of distance. The sensitivity is the ratio of number of expected photoelectrons between data and simulation. The sensitivity of the optical modules is still coupled to the ice model. Of greater interest is the fact that for AHA, this coupling is as strong as for the Millennium ice. The two plots are shown in Figure 5.4.

The sensitivity varies with depth on a scale similar to the variations in scattering coefficient. Although the degree to which the sensitivity is coupled to the ice model is minor, it was expected that the deconvolving of the smearing effect would decouple the OM sensitivity from the ice model significantly more than it has. It is now thought that systematic problems arising from the method used in determining the ice model are not to blame. This suggests that no further improvements in the ice model will be made

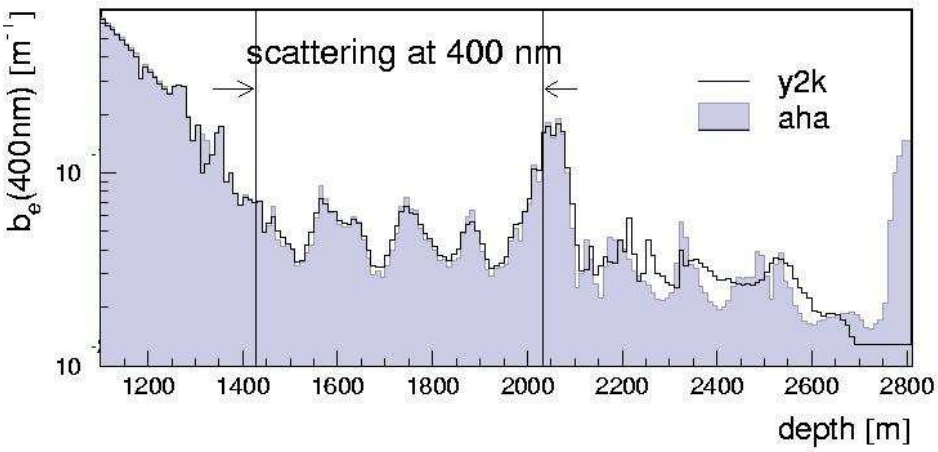

(a) Scattering

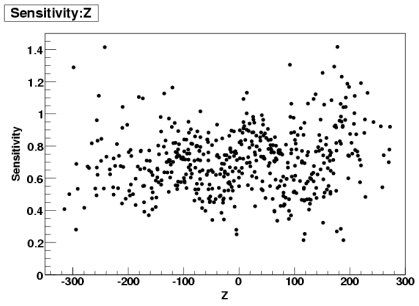

(b) Millennium Ice

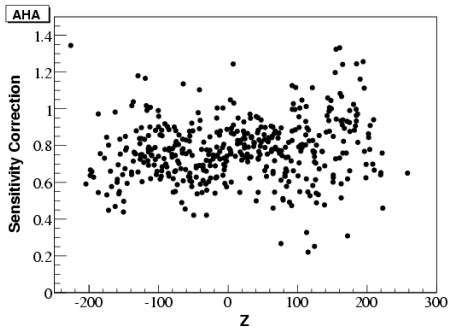

(c) AHA Ice

Figure 5.4: OM Sensitivity vs Depth

Plots produced by Jim Braun showing that both Millennium (b) and AHA (c) ice appears to have optical properties that are coupled to OM sensitivity. The sensitivity varies with depth in a similar way to the effective scattering coefficient in (a). The centre of the AMANDA array, the coordinates of which are used in the distributions shown in (b) and (c), is at a depth of 1730m.

using in situ light sources alone. It is possible, as we discuss in Section 6.5, that with the added information gleaned from dust logs and ice cores about the finer structure of dust layers, along with in situ light source data and some additional assumptions about the composition of dust, we can build a more accurate ice model.

5.3 Solutions

The resolution of the depth dependant discrepancy between simulated and observed data is a major issue for the IceCube collaboration. If the search for high energy extra galactic neutrino sources is to prove fruitful, it is necessary for simulation routines to be as accurate as possible. While the discrepancy between simulated and observed data remains, it is clear that not all of the pertinent physics is being accounted for in the simulations. A number of possible avenues for investigation are discussed below.

5.3.1 Highly Absorbing Layers

The problem may be that there are actually features beyond the resolution of the current ice models that are affecting the way that light propagates. In this thesis we are primarily concerned with adding thin absorbing layers into the ice; effectively cutting out the flux of photons through dusty layers. In his thesis [27] Marek Kowalski showed, in an AMANDA simulation chain before the advent of Photonics, that creating layers that were essentially opaque to photons in the known dusty areas of the detector significantly reduced the discrepancy between peaks in the Monte Carlo and data COGz distributions. Using the 3 dustiest regions as defined by the previous generation of ice model, he removed hits originating from two particular event types:

- If the light emitted by a secondary particle has to pass through a layer, or comes from within a layer, to get to an optical module outside of the layer, the hit is removed.
- In the case of the emitting particle being a muon, the origin of the light is assumed to be the point of closest approach of the muon to the triggered optical module, and the same conditions as above are applied.

It is clear that such an approach is not physically feasible; the special MC simulation didn't allow any photons to pass through the dusty layers, which is probably an excessive restriction. At that stage Photonics had not been used and it was believed that when Photonics was implemented with its heterogeneous description of the ice it was likely to correct such issues as the COGz problem.

It is this previous work that motivates the work of this thesis. Instead of entire sections of the ice being completely opaque to photons propagating through the medium, we trial inserting thin, highly absorbing layers into the current ice models in the known dusty

areas. Such layers are physically feasible. The suggestion of thin layers of volcanic ash having been deposited is a well researched topic. Ice cores from other parts of Antarctica suggest the presence of such thin layers [11–13] and it is well known that volcanic ash has a low albedo - absorbing light particularly well while scattering very little.

5.3.2 Alteration of Binning

A second possibility is that the binning size used in other aspects of the photon table production leads to the discrepancy. We have not investigated these possibilities in this thesis, but discuss them now for completeness. There are two areas that could benefit from a revision in the way that they are binned; the binning within Photonics tables and the distance between sources.

Considerations

Although a finer binning is likely to improve some aspects of the simulation, there are drawbacks to such an approach. With smaller bins describing the same physical space, it is easy to run into problems with table size, for a finer source depth spacing we would have far more tables to deal with, while a more detailed description of the medium would require increases in the time required to generate a set of tables. The latter problem is not of any great concern, as usually tables are not produced on a regular basis, but rather a production set is generated for use in the simulation chain by the entire collaboration. Studies have been carried out by Kyle Mandli for the AMANDA collaboration [31] that show that given the current ice model, the binning used is the best compromise between size and precision. Table 5.1 shows various sizes of level 1 tables for varying degrees of detail in binning in position and time variables.

Photonics Binning

It is possible that there are problems originating from the low level binning of Photonics tables in the various dimensions. Currently it is normal to use quadratically increasing bin sizes emanating out from the source of light. This makes sense for position and timing bins close to the origin, however it is clear that we lose detail as we move away from the source of the photons.

In this thesis we take the standard Photonics binning to be that of the latest mass production tables created for the AHA model. Table 5.2 indicates the binning used for various coordinates within individual level 1 tables. One can see that for if we were using

ρ	ϕ	z	t	size
50	18	105	90	33 MB
45	16	95	80	21 MB
40	14	85	70	13 MB
35	12	75	60	7.3 MB
30	**9**	**65**	**50**	**3.4 MB**
25	8	55	40	1.7 MB
20	6	45	30	644 KB
15	4	35	20	176 KB

Table 5.1: Table size compared to binning depth

Size of each level 1 Photonics table for given bin sizes. The current standard (bold type), shown to be a good mixture of small table size and suitable depth of detail in resulting simulation, is that used for current production tables. All tables generated with limits as described in Table 5.2.

linear scaling of bin size, for all bins it is possible that more than one IceCube DOM, which are on average 17 metres apart, could coexist. This means that as far as Photonics sees, these DOMs see the same amount of light. On closer inspection we find that since it is standard practice to use quadratic binning of ρ and z, it is not possible for two DOMs to coexist in the same spatial bin until distances of approximately 120 metres are reached. It seems that while we bin distances quadratically it is unlikely that such an effect will be of any consequence; by the time that the light has traversed such distances, the difference in light between DOMs that are in close proximity will be negligible.

Dimension	Bins	Recordable Limits	Active Limits
Radial, ρ	30	$0 \rightarrow 580$m	$0 \rightarrow 680$m
Azimuthal, ϕ	9	$0 \rightarrow 180\,^\circ$	$0 \rightarrow 180\,^\circ$
Zenith, z	65	-580 $\rightarrow$ 580m	-680 $\rightarrow$ 680m
Timing, t	50	$0 \rightarrow 7000$ns	$0 \rightarrow 7000$ns

Table 5.2: Photonics Level 1 Binning

Level 1 Photonics table spatial and timing binning, as taken from AHA production table set. Quadratic scaling is applied to radial, zenith and timing bin spacings so that more detailed description of distribution of light is obtained closer to the source. See Appendix A for a more in depth list of table properties used.

Source Depth Binning

The negative effect of combining Čerenkov sources separated by 20m distances[1] to make muon tracks is one that could be a contributing factor to the mis-reconstruction of muon tracks.

One would assume that it is not ideal to create a description of a continuous track from point sources separated by as far as 20 metres. This may well be the case in the range of depths where the ice has dramatically varying parameters. At the start of this chapter we discussed a possible reason for the discrepancy in COGz plots. Namely, that simulated downgoing muons are mis-reconstructed as travelling upward. While we represent light from muon tracks by the sum of Čerenkov sources spaced 20m apart, we might not be gaining full advantage of the ice model, currently binned in 10m depth intervals.

The light that is received below a particularly dusty layer is the sum of the light that has reached that position from each of the Čerenkov sources along the track. This means that there may be no contributing light sources within the layer of dust, which would certainly create a difference between simulated and real hits, as in the detector, light is emitted continuously along the muon track. One logical direction in which to proceed would be to generate sources closer together in the areas in which ice properties are quickly varying, while leaving them even more sparse than normal in the large expanses of clearer ice that exists below the fourth major dust peak.

Currently we have our sources at a spacing of 20 metres in vertical separation. There is a possibility that we are losing some detail in our simulations by not being able to perfectly describe an electromagnetic shower that occurs between depths at which we have simulated them. Consequently, the ice properties which currently have a 10 metre depth binning are not taken full advantage of. Since cascades are relatively well simulated compared to muons, it is likely that these effects can be ignored.

Variable Binning

As mentioned above, one potential avenue for further research is the possibility of finer binning detail in regions where the rate of change of ice properties is greater. In the deeper, cleaner ice, we may not need as fine binning to describe processes to a similar detail.

If it is assumed that ice properties do not change very much, for example, in the

[1] For muon tracks which are not entirely vertical the physical distance between the Čerenkov emitters on the track is greater than 20m.

deeper ice then we could get away with integrating over sparser individual Čerenkov sources to build muon tracks. Conversely, where we require greater depth of detail, we could integrate over sources placed closer together. This would result in the need for additional weighting depending on the sparseness of the contributing Čerenkov sources.

Alternating the size of the bin at which the flux from an individual photon is recorded depending on the rate of change of the ice properties is an achievable step. One could setup a predetermined binning scheme that varied with the ice properties so that there were no further computational steps, and Photonics could process photon propagation as normal. The advantage of variable binning is likely be minimal due to the spacial resolution of the IceCube array; DOMs are 17 metres apart and for relatively short source-receiver distances the current detail of binning is sufficient.

A counter argument to the need to vary the bin size, in particular the source spacing of Čerenkov emitters, is that the properties of the ice do not appear to vary on a scale that is any smaller than the current 20 metre source spacing. Unless the resolution of dust peaks is improved, variable binning is probably unnecessary.

5.3.3 Simulation Chain Alterations

Another possible source of the problem of mis-simulated muon tracks is the simulation itself. If not all of the pertinent physical processes are accounted for in the simulation of photon propagation or the propagation of muons through the medium, then this could be the origin of the problem. If the underlying model of the propagating medium is not to blame for problems originating from description of propagating Čerenkov light from particle tracks, then it is possible that the description of these particle tracks is incorrect in our simulations. This seems from casual observation to be extremely unlikely, considering the coherence that the unsimulated peaks and valleys have with known fluctuations of scattering and absorption. We therefore choose to focus on the proposition of Section 5.3.1 for further analysis.

Chapter 6

Insertion of Thin Absorbing Layers

Motivated by Marek Kowalski's work, as mentioned in Section 5.3.1, we seek to investigate whether thin absorbing layers can reduce the discrepancies that we see between experimental data and simulation.

6.1 Model Development

The first steps are to decide where to insert these layers, how thick they are to be, and what changes should be made to the optical properties in the layers. As a starting point, it was decided to use the Millennium ice model since the AHA model was not completed until midway into the thesis research period[1]. As demonstrated in Figure 5.1, the AHA model represents only a limited improvement as far as simulation of muon tracks is concerned, so the decision to keep the Millennium model as a base for changes is reasonable.

Photonics allows the user to manipulate the description of the medium in any way, so long as it does not vary horizontally. Thus it is particularly simple to insert a new layer into the ice model. As we are only interested in highly absorbing layers, we take the properties of the existing layer, into which the thin layer is to be inserted, and adjust the absorption. For simplicity, we chose to simply increase absorption by a given factor within this layer. Once a model was decided upon, a complete set of Photonics tables was generated for the model, as described in Section 4.1.1. Due to time constraints, the tables that we generated are of relatively low statistics; that is, the number of photons propagated through the ice for each source is only 600,000, rather than the 60,000,000 of

[1]For the latter two models, the description of the clearer ice below the last large dust peak was taken from the AHA model, however above this the underlying ice model in which the dusty layers were placed remained the Millennium model, for continuity's sake.

the production models. The effect that these lower statistics has on the analysis will be discussed later.

The process which lead to the following three main models included several attempts at including only very small increases in absorption in only two or three layers of thickness on the order of a centimetre. It appeared from preliminary observations that the effects of such layers were not easily detected since the properties of the propagating light tend to be smeared out as scattering processes lead to photons spending time in surrounding layers, as is described in Section 3.4.3. Consequently more drastic alterations to absorption were tested. The analysis involved simulation of background muon activity within each model and observation of timing distributions for various sources.

6.1.1 Model 1

The first model for which an entire set of Photonics tables was generated was a trial model to determine the ease of inserting layers, and also to gauge whether increasing absorption by a factor while making the layer thinner by the same factor would have any discernible effect. Within each layer of the base ice model, the y2k model, a layer of one metre thickness, and ten times the absorption coefficient of the layer in which it resided was inserted. Clearly this model does not represent the actual depth dependent ice properties but as explained, was intended as a test model.

6.1.2 Model 2

Model 2 was intended to be a more realistic model of ice layers. In this model the positions in which layers were placed was confined to areas in which the absorption coefficient at 400nm is greater than or equal to 0.01 in the Millennium ice model. Such a limit was chosen as a guideline as it results in a more realistic number of thin layers[2], and it also follows the work described in Section 5.3.1. This results in 32 layers in total, in regions defined in Table 6.1.

In each of the above layers, the absorption coefficient was increased by a factor of ten, with layers remaining at one metre thickness.

[2]In Section 6.5 we discuss further developments that could be made to produce an even more realistic layering.

Region	Layers
-145.4 → -15.4m	13
54.6 → 84.6	3
304.6 → 404.6m	10
174.6 → 234.6m	6

Table 6.1: Model 2 layer positioning
Measured in IceCube coordinates, the zero point of which is at a depth of approximately 1950m.

6.1.3 Model 3

The third model is identical to the previous except that it has layers of only ten centimetre thickness, with absorption coefficient 100 times greater than that of the layer in which it is embedded. The reason for this change, rather than an improvement in statistics or a different layering approach, is to investigate whether we retain any effects seen in the second model when the layers have a more physically realistic thickness. It is extremely unlikely that one metre thick ash bands exist anywhere at the depth of the detector at the south pole, however studies from other parts of the Antarctic have shown the existence of ash bands of thickness on the order of millimetres to tens of centimetres [11].

6.2 Initial Analysis

In addition to simulated data, time distribution curves offer a further indicator of the potential that an ice model has to represent reality. Since the y2k and AHA models were built by analysing the distribution of photons emitted by a given source in a layer, the time distribution plots that they produce should be reasonably accurate. In this section we carry out some auxiliary studies based mainly around time distributions in the generated models.

6.2.1 Test of Statistics

A test that was carried out after the simulation was to provide an indication of whether our use of such low statistics in photon tables (600,000 instead of AHA's 60,000,000) is likely to have caused any major problems. For this small study, we simulate an isotropic source of light at a position in the clear, deep ice of -710m in IceCube coordinates with

photon densities of 600,000 and 60,000,000 for y2k and Model 1 ice. This depth is directly between two absorptive horizons in the Model 1 ice. Using a script that employs PSI, we generate timing distributions for various source receiver distances both vertically and horizontally and observe the difference between the higher and lower statistic tables. In Figure 6.1, we show four of these comparisons.

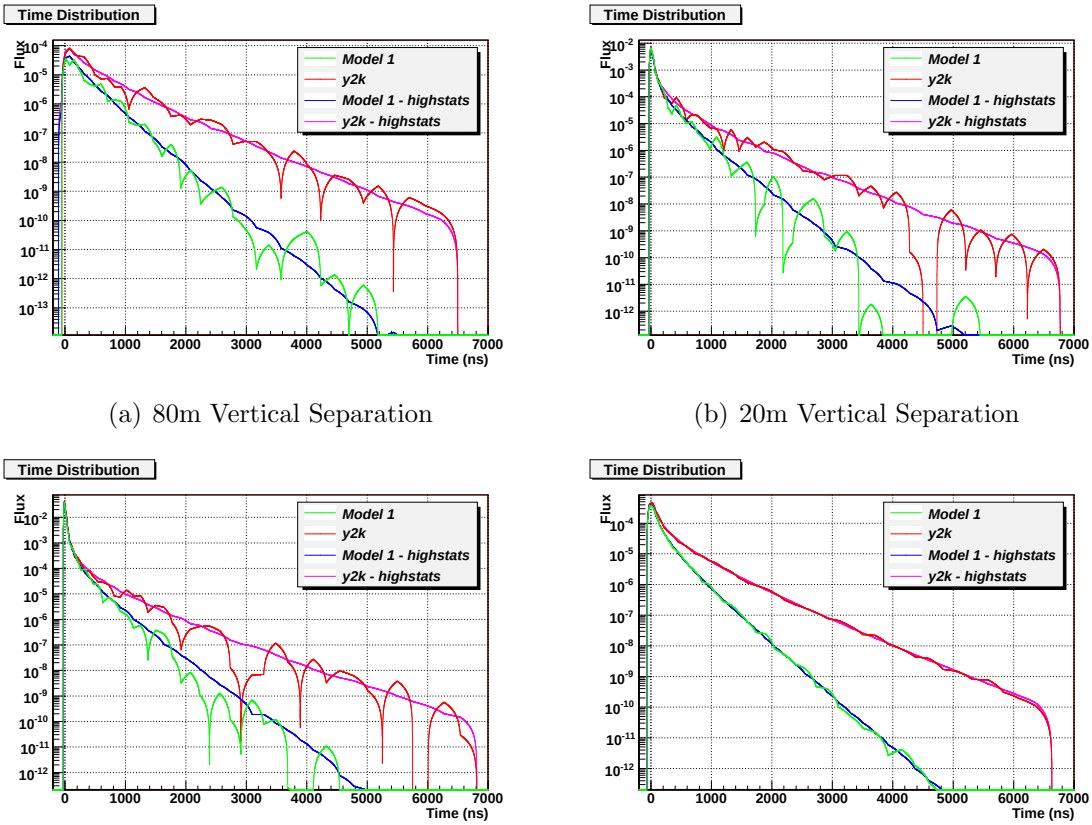

(a) 80m Vertical Separation

(b) 20m Vertical Separation

(c) 10m vertical separation

(d) 50m horizontal separation

Figure 6.1: Time distribution comparison for isotropic sources of varying statistics Here we compare the resulting time distributions from Photonics tables generated at -710m using 600,000 and 60,000,000 photons with different receiver-source orientations.

It is clear in these plots that the accuracy that is lost through reducing the statistics in each Photonics table is in fact significant. The reason that the time distributions of low statistic horizontal source-receiver configurations show so much less deviation from their high statistic partner than those of vertical configuration is a remnant of the binning system. Vertically each Photonics table has 65 bins in a 1160m distance centred on the source. The radial dimension has 30 bins over a distance of 580m. The bin sizes increase with distance from the source, so that the bin at, for example, 50m radius stretches from approximately 41m to 52m, whereas the bin closest to the source extends from the centre

to a radius of 64cm. In the vertical direction, we also have quadratically increasing bin size so that the closest bin to the source is 32cm deep, while a bin at 50m vertical distance stretches from approximately 50m to 61m. The depth of the bin at 50m horizontal distance is approximately 11m - the same as the bin at 50m vertical distance. Photonics bins in cylindrical shells split into azimuthal pieces. In the binning we have used, each shell is split into 18 sections azimuthally. We can easily calculate the volume of the two bins in question by calculating the area of the cylindrical shell for the radial direction and the vertical thickness at each bin.

We see that for the bin 50m radially separated from the source the volume is

$$\frac{0.32 \times (\pi \times 52^2 - \pi \times 41^2)}{18} \approx 57\text{m}^3. \tag{6.1}$$

This is approximately 75 times that of the bin at a 50m vertical distance

$$\frac{11 \times (\pi \times 0.64^2)}{18} \approx 0.8\text{m}^3. \tag{6.2}$$

Photons are isotropically distributed, however a cell of smaller volume is more likely to receive no photons in a given time bin than a larger cell. Since PSI interpolates over neighbouring bins when calculating time delay information, the dips in the distribution of Figure 6.1 are caused by bins close to the desired observing distance having received a small flux of the outward propagating photons compared to other times. This explains the discrepancy between the distributions when the source is observed from a horizontal as compared to a vertical distance. If for observing points that are vertically separated from the source we offset the observation point radially by a small amount, the distribution begins to smooth out as shown in Figure 6.2

We see that lower statistic tables have time distribution curves that, despite showing increased noise, still follow the same curve as those of higher statistics. Figure 6.3 shows that the probability distribution for the position of photons, as it evolves over a short time period (100 - 500ns). This shows very little deviation between the differing statistics

The discrepancy that we see in Figure 6.1 is an effect caused by the way that we set up the binning in Photonics. This shows that the binning system is not ideal for isotropic sources. Since the distribution of light from a shower is roughly spherical in appearance in the detector, they may also be affected by this, however the problem is only evident for low statistic tables so the binning requires no alteration for production level tables. Any further studies in this direction should use higher statistics.

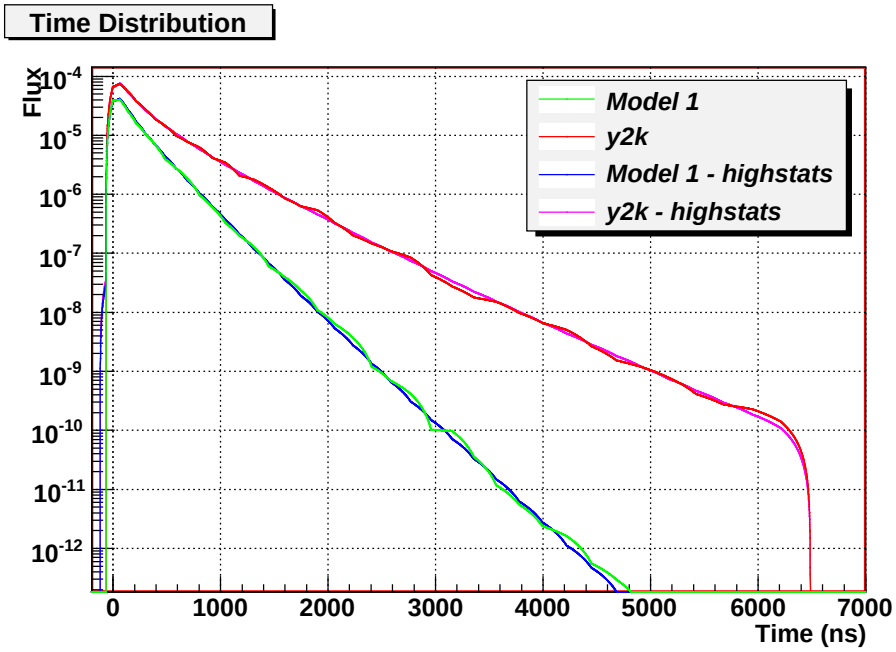

Figure 6.2: Time distribution for isotropic source viewed from offset vertical position Here we show that by slightly offsetting the observer position radially, the distribution begins to smooth out. This is the same isotropic source viewed from a radially offset 80m vertical distance.

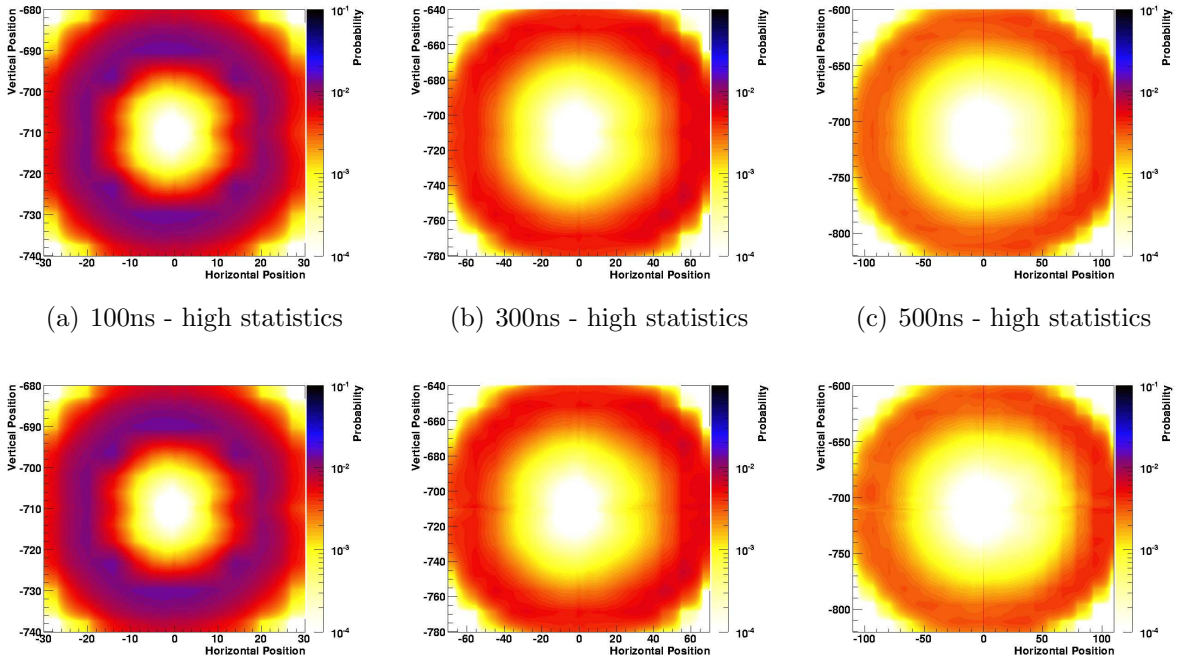

(a) 100ns - high statistics (b) 300ns - high statistics (c) 500ns - high statistics

(d) 100ns - low statistics (e) 300ns - low statistics (f) 500ns - low statistics

Figure 6.3: Evolution of probability distribution over time

Probability distribution about the central light emission for high statistics (top) and low statistics (bottom) photon tables. The distribution gives an idea of the most likely position of the photon cloud at each time after the source is initiated in a given x-z slice of the ice centered about z=-710m. Note the differing distance scales.

6.2.2 Effect of Altering Optical Properties

In the next section we will examine how time distribution curves are affected by the presence of thin layers. To gain an idea of how changes in scattering and absorption affect these distributions we create photon tables of high statistics for a homogeneous ice description (so depth is unimportant), and then change absorption and scattering. Figure 6.4 shows the variation in time distribution curve for each of 6 variations on the standard homogeneous ice.

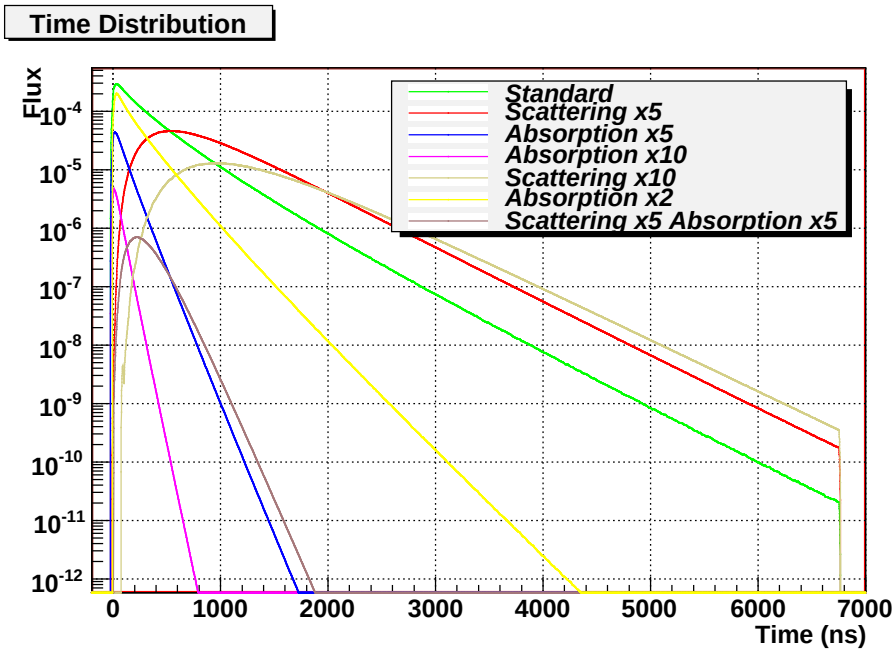

Figure 6.4: Comparison of effects of varying optical properties

As is evident above, a higher absorption coefficient results in a shorter time distribution while higher scattering results in a broader peak.

We find that, as would be expected, altering the absorption length, while not affecting the peak in the time distribution curve dramatically reduces the length of time that we are able to see photons that originated from the source in question. On the other hand, decreasing the effecting scattering length means that photons scatter on a more regular basis and the average time of travel is not defined as sharply. When observing distributions from our models we expect that we will likely see changes that result in a similar peak, but a steeper decline since we only alter absorption.

6.2.3 Impact of Thin Layers

Any changes to the shape of the light distribution curve over time will only be due to changes in absorption since this is the only parameter that we vary. If however the layers are sufficiently thin, their effect might be smeared out when we observe a close by source from a suitable horizontal distance. The process of smearing was described Section 3.4.3. The basic idea is that photons will spend little time in the absorptive layer due to scattering processes and therefore sample the optical properties of the surrounding layer more. This is described in more detail in Given the method in which the AHA and Millennium models were determined using in situ flasher data, they are taken to represent good fits to light source data in the actual ice. Therefore, if our models are to provide a useful route forward, they should show similar time distributions to those of the established models. Here we look at two different scenarios of source-detector pairings; those in between two layers and those that have only one such layer within any reasonable distance.

For the first scenario we choose to test for all models except Model 1, by observing time distributions for source receiver pairs within the 10 metre layer from -95.3m to -85.4m in IceCube coordinates. There is a thin layer at each boundary of this layer, which resides within the major dust peak. We place sources at depths of -95m, -90m and -85.7m, with the lowest and highest of these being almost in contact with their respective thin layer boundaries. Figure 6.5 shows the time distributions for the three depths, at which the source and receiver pairs are separated by 50m.

It would appear from observation of the plots in Figure 6.5 that within the 10 depth interval between thin layer insertion depths, the time distribution curves show very little variation. The fact that we see such a discrepancy between the standard ice models and Models 1 and 2 would indicate that for the layers that have been inserted, smearing is not washing out the effects of the layer. This could be explained by the fact that the effective scattering coefficient is approximately 0.2 in this dusty part of the ice which corresponds to a geometric scattering length of approximately 1 metre. This means that light scatters more often so photons that pass through the absorptive layer have more chance to scatter back toward the detector within the 50m observing distance. This explanation implies that for ash layers that appear outside of the known dusty ice, smearing may play a larger role. Such layers are not included in this thesis, however it may be a useful avenue for further research once actual positions of ash bands are known to more detail. The effect seen in Figure 6.5(f) that sees a difference for Models 2 and 3 is most likely due to the fact that as Model 2 has absorptive layers of 1 metre thickness, the source and receiver

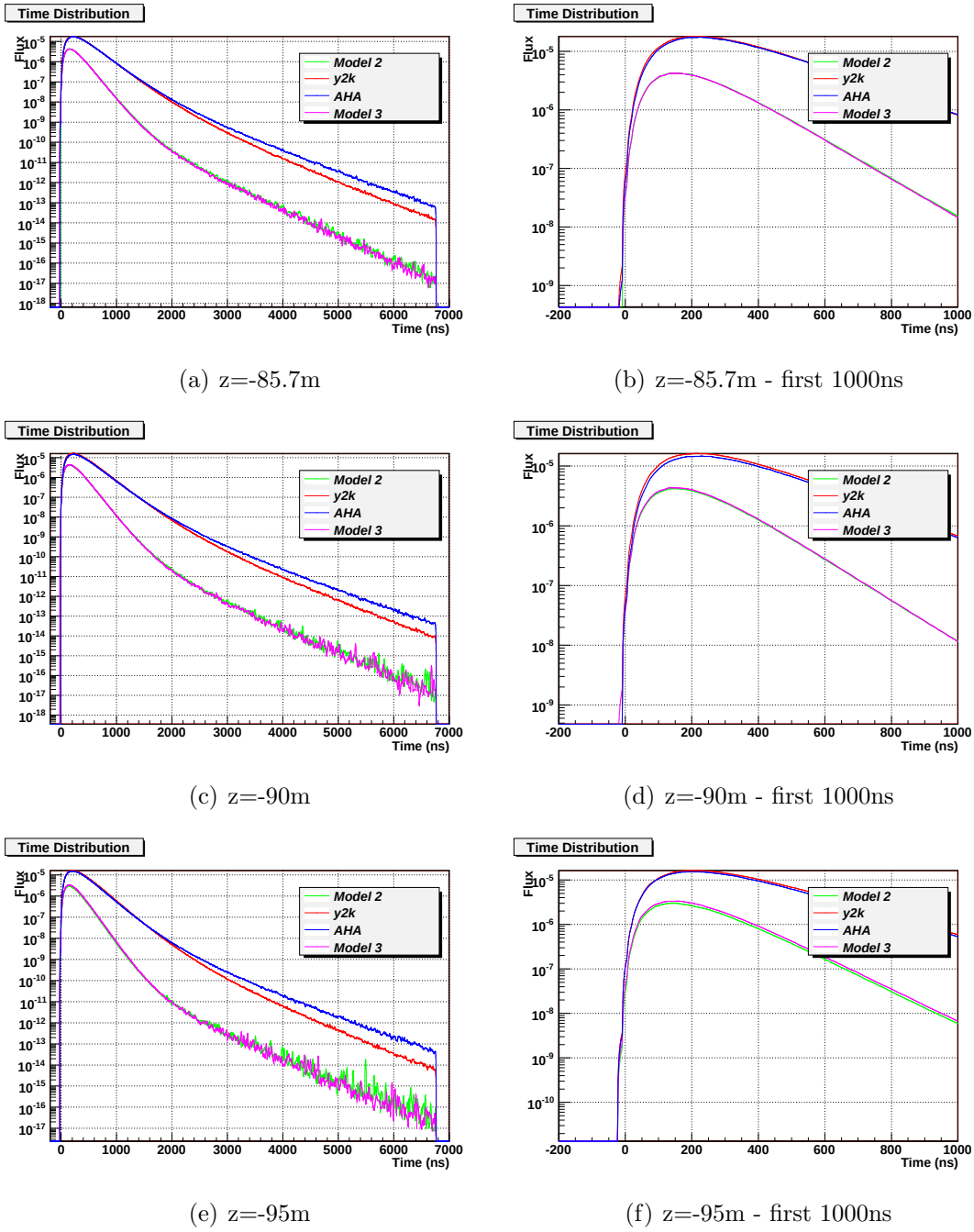

(a) z=-85.7m

(b) z=-85.7m - first 1000ns

(c) z=-90m

(d) z=-90m - first 1000ns

(e) z=-95m

(f) z=-95m - first 1000ns

Figure 6.5: Comparison of depths between thin absorbing layers
Here we plot the time distributions for varying source-receiver depths between two absorbing layers. Model 3 is obscurred by Model 2, indicating that the change in thickness has little effect.

are in fact within the layer, whereas for Model 3, they are very slightly above.

The second scenario that we test is that of a layer, in this case at approximately -25m in IceCube coordinates, with a significant distance before the next thin layer. We create photon tables for an isotropic source at varying distances from said layer, and observe the

effect that the layer has on the distribution. The layer at -25m is right on the edge of the lowest large dust peak, so there is a possibility that photons that pass through the first thin layer, may also probe further absorptive layers; as we move the source further from the layer, we should see less of a contribution to the overall absorption by these layers.

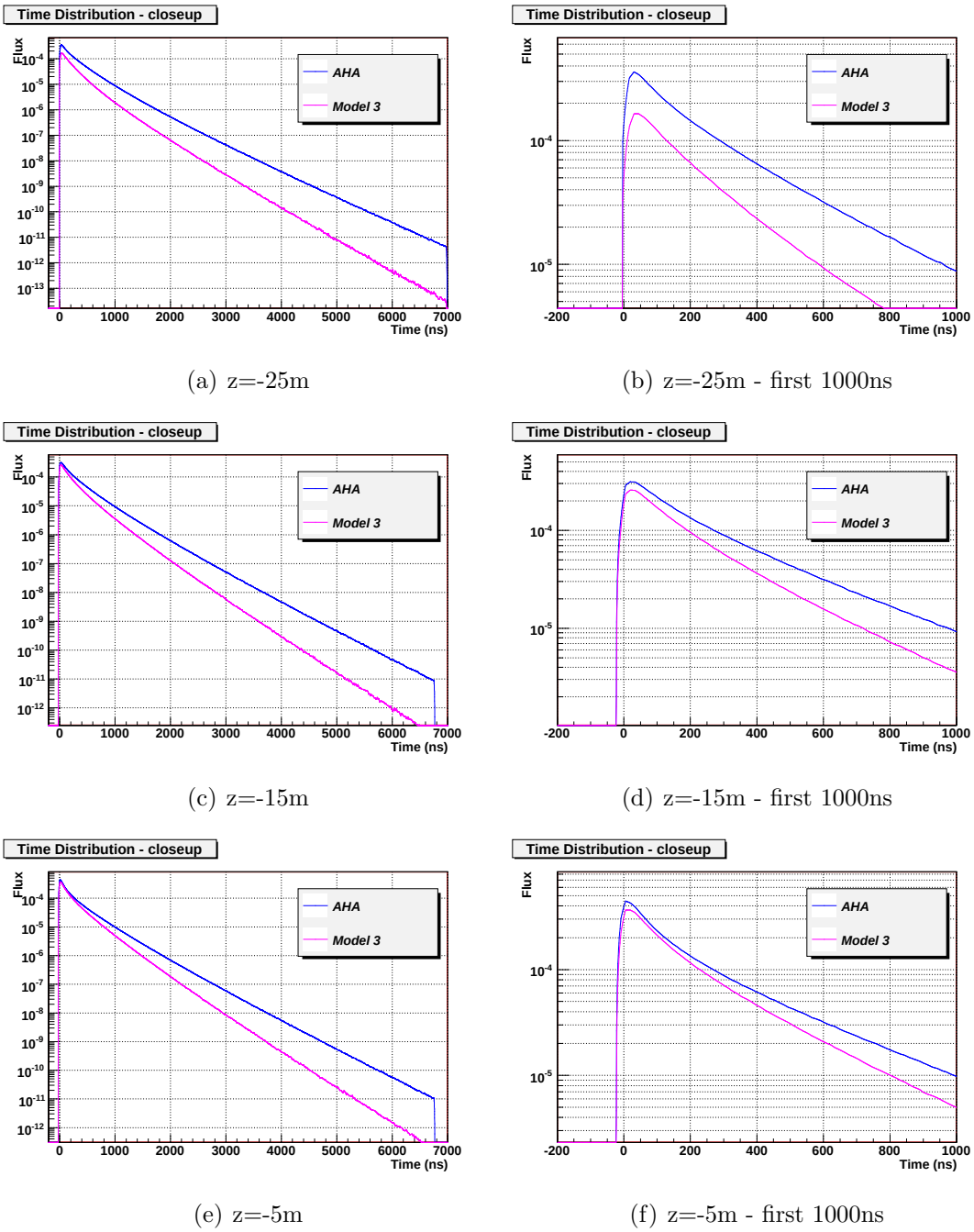

(a) z=-25m

(b) z=-25m - first 1000ns

(c) z=-15m

(d) z=-15m - first 1000ns

(e) z=-5m

(f) z=-5m - first 1000ns

Figure 6.6: Comparison of depths near a thin absorbing layer
Here we plot the time distributions for varying source-receiver depths in the vicinity of an absorbing layer at approximately -25m in IceCube coordinates.

The plots shown in Figure 6.6 confirm that as we move the source further from the

absorptive layer, the effect of the layer is reduced. Unfortunately, we still see a significant increase in the gradient of the time distribution curve for all distances, indicating that effect of layers of the configuration that we have used is not smeared out as was hoped. Despite the layers being of some distance from the source, the distributions still show a reduction in light, due to the increased absorption of the layers below.

6.2.4 Overall Absorption

One striking feature of the plots in Figures 6.5 and 6.6 is that the overall absorption is clearly too high in the new models. The timing distribution drops off at a much earlier time than for the existing models and, since the peak is of the same shape, the discussion in Section 6.2.2 suggests that differing overall absorption creates this discrepancy.

We make a crude estimate of the average absorption of the entire 10 metre ice layer to be $\frac{tA_1+(T-t)A_2}{T}$, where t is the thickness of the thin layer, $T = 10$m is the thickness of the entire layer, A_1 is the absorption of the thin layer and A_2 is the absorption of the rest of the 10 metre layer. Model 3, for example, with $A_1 = 100a$, $A_2 = a$ and $t = 0.1$m, where a is the original absorption coefficient for the entire layer, we have an average absorption of $1.99a$.

This means that the models we have used may not be testing the effect of the thin layers that have been inserted, but rather a doubling of the absorption coefficient over the whole layer. As a test of this, we make some tables with an isotropic source located at $z = -90m$, varying the ratio of the absorption in the thin layer to the absorption in rest of the 10m layer. The ratios tested are summarised in Table 6.2

Test Model	Absorption of thin layer, A_1	Absorption of bulk of layer, A_2	Averaged absorption
Model 3	$\mathbf{100a}$	$\boldsymbol{a}$	$\mathbf{1.99a}$
A	$100a$	$0.5a$	$1.495a$
B	$100a$	$0.1a$	$1.099a$
C	$100a$	0	a
D	$90a$	0.10101...	a

Table 6.2: Models to test effect of change in average absorption
All models are created with Model 3 (in bold) as a template. The thin layer is left at 10cm thickness.

From the Photonics tables that are generated we determine the time distribution and compare. As can be seen in Figure 6.7, with a decrease in overall absorption we see a higher light flux at later times than for models with higher absorption. An unexpected result is that of Model B. Despite the overall absorption being greater than the underlying y2k model, the model still shows an increased flux over time. This is an indicator that there is potential that there are thin absorptive horizons present in the ice that the current models do not represent correctly. It is possible to add overall absorption to a

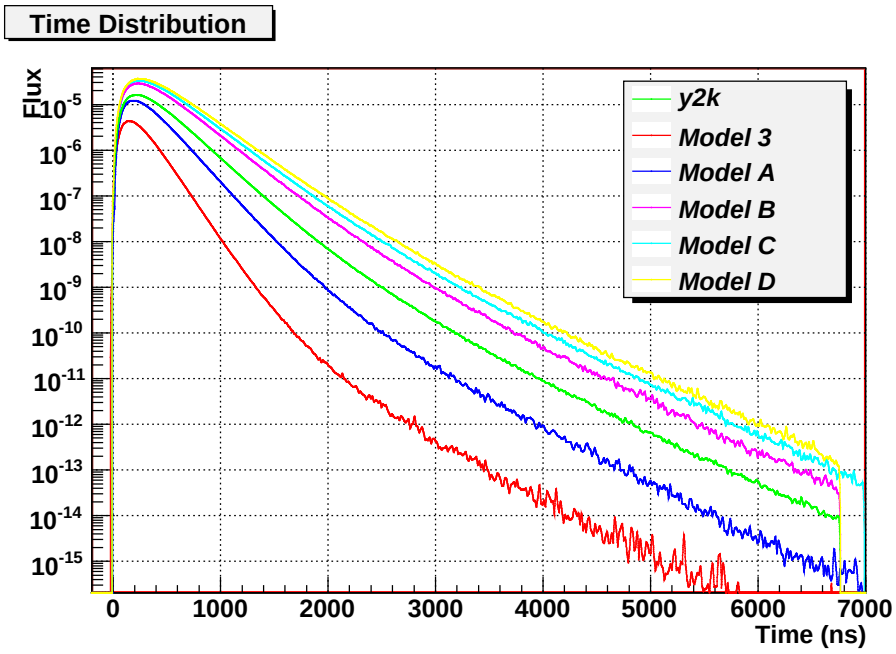

(a) Varying absorption

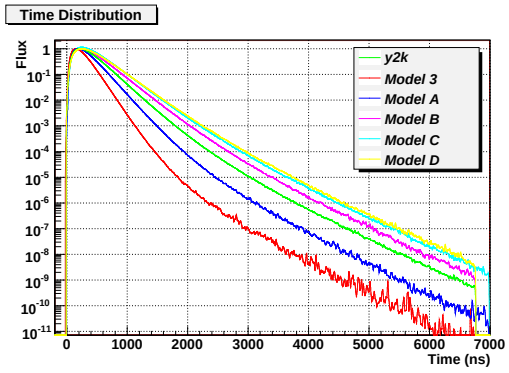

(b) Varying absorption - normalised

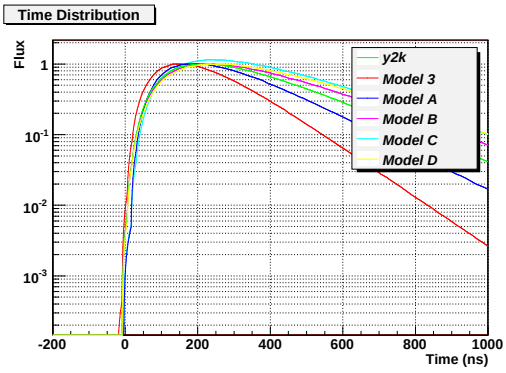

(c) Varying absorption - normalised

Figure 6.7: Variation of absorption according to Table 6.2
The green line shows the underlying Millennium ice model, while the red line is Model 3. It appears that some reduction in the absorption of the balance of the 10m layer should have been made so as to leave the average absorption of the entire layer closer to the original absorption.

layer without reducing the flux of photons. The fact that the flux from Models B, C and D is greater than that of the y2k ice is due to the fact that when the absorption is concentrated in a thinner portion of ice, the photons spend less time under its effect, as they tend to scatter out of the layer, spending more time where the absorption is lower.

In the time period associated with this thesis, the allocation of computing resources resulted in a limited available time to carry out simulation and reconstruction. This

resulted in test models being chosen before the tests described in this section were carried out. Had the order been reversed, the models would have been chosen in accordance with the results of the above tests. The absorptivity of the balance of each 10 metre layer into which a thin layer is inserted would have been adjusted to account for the increase in overall absorption that the thin layer presents so as to match the light distribution of in situ sources. In any future endeavours in which thin layer insertion is proposed, it is suggested that time distribution tests be carried out to determine the viability of a model before background muon simulation is carried out.

6.3 Simulation Details

In order that the models for which photon table sets have been created can be compared to data and existing simulation, we must run through the standard simulation chain. We simulated atmospheric muons using pre-existing CORSIKA files configured for use in IceTray. We seek to simulate both single and coincident muons in the 22 string configuration of IceCube, IC22. Coincident muons are two (or more) downgoing muons that enter the detector in such a way that the light signature that is generated in the detector can not easily be separated into two individual tracks. Such coincident events can mimic up going neutrino events very well, so there is certainly a need to simulate their presence correctly so that they can be removed from a neutrino analysis.

Although it is important to simulate coincident muons as well as single muons in order that comparisons made to data are complete, we were not able to perform the reconstruction of the combined events before the end of this thesis. We rely on the fact that the rate of coincident muon events is approximately two orders of magnitude less than that of single muons. The results of simulation with only single muons from CORSIKA air showers is thus comparable to data at the level we are comparing.

After simulation we reconstruct using a simple linefit method, then write various results of the reconstruction to a ROOT file to be combined and plotted. We simulate with 20 CORSIKA files, each of which represents approximately 2.62 seconds of live time. These are relatively low statistics, however a need to produce simulation for all ice models tested on top of the already computationally intensive process of producing photon tables results in limited available time and computing resources. In any case, the simulated muon tracks that we have for the tested ice models are sufficient to provide an insight into differences that occur.

6.4 Occupancy Comparison

Upon completion of the generation of photon tables and, subsequently, the simulation of muon background within each model we are able to compare occupancy plots for each model. By retrieving data, both simulated and experimental, from the IceCube data repository we can compare the outcome to the established models. Figure 6.8, shows a comparison of the DOM occupancy for Models 2 and 3 with AHA simulation and observed data.

We see an increased agreement between simulation and data for the two models that we tested. As was discussed in Section 6.2.4, this change in occupancy could be purely due to the increase in total average absorption in the dusty layers. Although we therefore may not be testing the same effect as we set out to, the increased agreement with data indicates that there could be a need to further stretch the absorption peaks in the dusty areas. The increase in overall absorption would make the layers less transparent to photons, thus reducing the numbers of hits in the dusty regions. This explains the increased drop in occupancy over the same regions that the occupancy of experimental data drops.

A particularly interesting feature is that of the improved match in the deeper, cleaner parts of the detector. Simulations using the AHA model show poor agreement with experimental data despite the description of this deep ice being drastically cleaner than that of the Millennium model. The ice description for the deeper, cleaner part of the detector used in Models 2 and 3 was identical to the AHA description, so we would expect a similar occupancy in this region. However we must also take into account that when plotting, we scale by the rate of events. The rates are $\sim$515Hz for AHA simulation and only $\sim$350Hz for Models 1 and 2. Therefore the actual number of events in this deep ice is approximately the same for the three ice models as the ratio of occupancy for AHA and Models 2 and 3 at these depths is the same as the ratio of the simulation rates. We have created models that result in a larger difference between the peaks and valleys of the occupancy distribution. This results in the plots appearing to fit the occupancy of data better, however the rate is somewhat lower than that of AHA ice and this would also need to match the data.

We also note that the peak in occupancy for data around DOM number 50 is not as pronounced in the plot in Figure 5.1, produced by Jon Dumm using data from June as opposed to the data from September used in this comparison. The chosen data appeared to be a good representative to compare to, with no artificial light sources present in the detector. This is currently under discussion, with a possibility that it has to do with the feature extraction process.

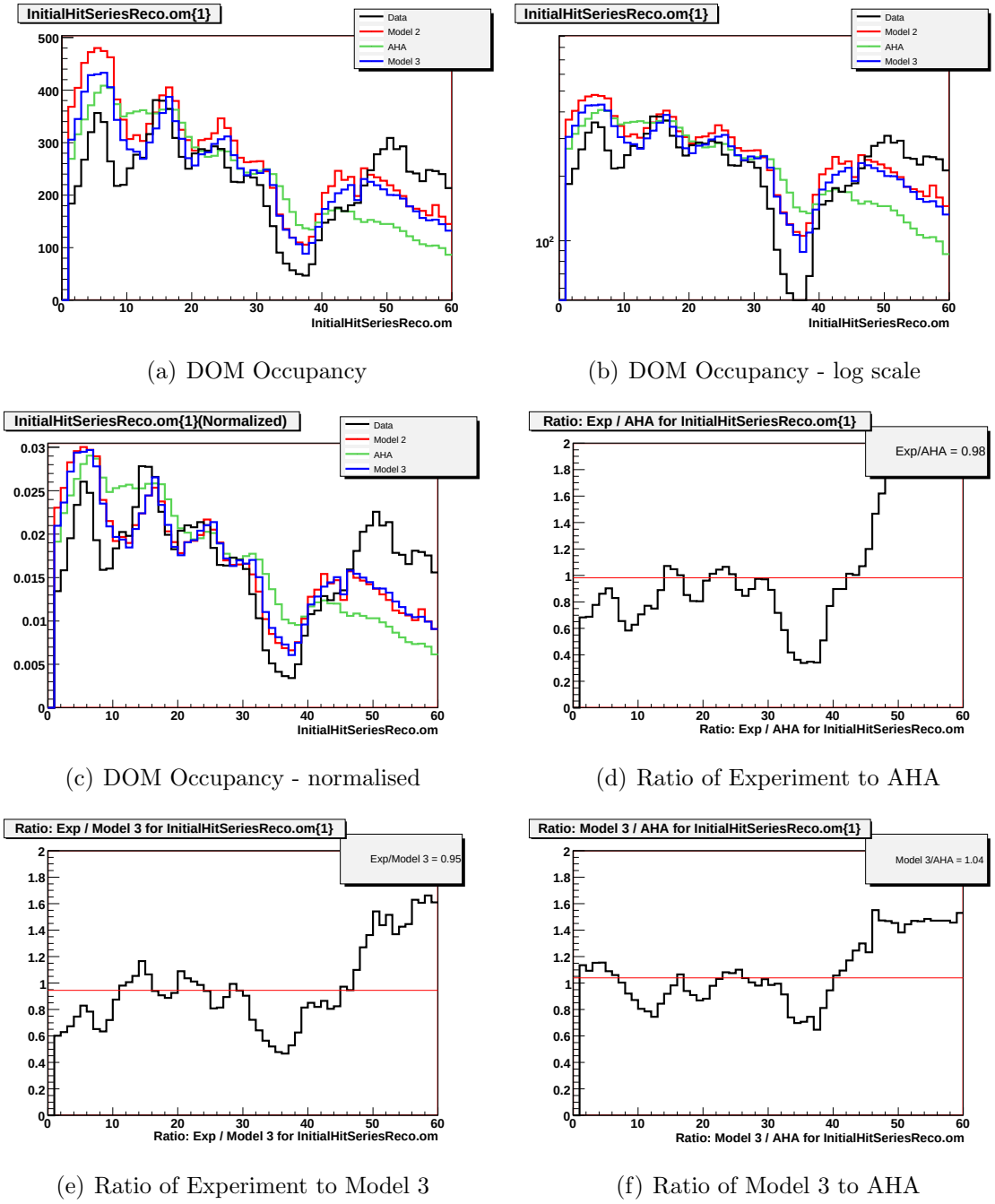

(a) DOM Occupancy

(b) DOM Occupancy - log scale

(c) DOM Occupancy - normalised

(d) Ratio of Experiment to AHA

(e) Ratio of Experiment to Model 3

(f) Ratio of Model 3 to AHA

Figure 6.8: Comparison of DOM occupancy
Here we show the difference between the DOM occupancy for simulated CORSIKA muons in AHA, Model 2 and Model 3 ice as well as the DOM Occupancy from the IceCube detector for a particular run.

6.5 Outlook

In this thesis we have investigated the consequences of inserting thin highly absorbing layers into the representation of the ice's optical properties used in the Photonics light

propagation simulation. These layers were inserted into the millennium ice model which uses ten metre thick vertical layers. This ten metre vertical spacing is finer than the seventeen metre vertical spacing of the IceCube optical modules and is as fine resolution as can be obtained using in situ light sources and detectors.

However, dustlogger data and measurements from ice cores are able to determine the dust profile to a much finer spacing. This profile may be able to be used, with some assumptions, to provide more realistic locations for the thin highly absorbing layers than those used in this thesis work. For example we have recently been provided with evidence of layers of volcanic ash of thickness on the order of 1 cm present at about five to ten different levels in the Polar ice [14]. This is fewer than the number of layers added in this thesis. Although it is unfortunate that time constraints did not allow us to trial placing thin layers using this information, it does offer an exciting avenue for further work. The apparent success of the simulations described in this thesis which produced occupancy plots with better agreement with data than the AHA model suggests that this is a useful line of investigation.

Chapter 7

Conclusion

Currently the IceCube collaboration uses a set of tables that describe the propagation of light from electromagnetic showers and muon tracks, generated using Photonics from the AHA ice model. This model, having originated from a study of the optical properties of the ice using in situ light sources is able to simulate point sources with high accuracy. It seems that the simulation of muon tracks using these photon tables is insufficient, as we see significant discrepancy between simulated and real data when observing the occupancy of DOMs in the detector in a given run, an effect that is seen in later stages of analysis as the COGz problem.

In this thesis we investigate the effect on the simulation of introducing thin, highly absorbing layers into the ice. Following the work of Marek Kowalski [27], it is thought that by reducing the amount of light that penetrates dusty regions of ice, we will be able to gain a better match to data for the occupancy of DOMs and through increasing the agreement in this lower level of data processing, simulated background will better match data at the later data reduction levels also.

In Chapter 6, we introduce three ice models, each with thin absorptive layers inserted in slightly differing configurations. The third of these has layers of 10cm thickness and absorption coefficient 100 times that of the layer in which they are embedded. This is on the order of size and relative absorptivity seen in volcanic ash layers in Antarctica, hence is it feasible that such layers actually exist within the IceCube detector.

By simulating a suitable background of downgoing CORSIKA muons using the IceCube software framework, IceTray, we are able to compare occupancy plots with those of simulations with the standard AHA model and data taken from the detector. The results, presented in Section 6.4, show a significant change in occupancy. We see a closer resemblance to the occupancy of the real data than that for AHA ice, indicating that

perhaps the AHA model needs to take a greater account of absorptivity.

It was expected that the contribution to horizontally observed time distributions of thin absorptive horizons in the ice would be smeared out, however plots presented in Section 6.2 show that this is not the case. This may be due to the number of layers, or possibly that the layers are too thick. A potential flaw in the method presented is that the overall absorption of each ten metre layer in which a thin layer is located is higher than it was previously. This is discussed in Section 6.2.4, and we conclude that in order that the time distribution match more closely with the base ice model's, the average absorption needn't be exactly the same as before but some alteration is required.

The improved match to data that the occupancy plots show in Section 6.4 indicates that not all absorptive features are accounted for in the current model. Finally, the results of Section 6.2.4 indicate that in future investigations of this nature in which thin absorptive horizons are included in the description of the ice, this inclusion should be accounted for by altering the absorptivity of the balance of the layer.

Appendix A

Additional Binning Information

This appendix includes further details of the set up of level 1 and 2 Photonics table geometry. The depths here are given in the coordinate system of the ice file, which is that of the IceCube Detector. We show the settings that are used in the Perl script that generates a driver file for each table that needs to be generated.

External Settings

The following settings describe the depths and source axis angles used for point source table generation (Čerenkov cone emitter or EM shower)

```
z_low  =  -800;  # lowest source position
z_high =  800;   # highest source position
z_step =  20;    # distance between sources
a_low  =  0;     #
a_high =  180;   # source axis angles
a_step =  20;    #

nph =  600000;   # number of photons to propagate
```

Internal Bin Settings

The following are the settings required for each point like Photonics table.

```
1     # Verbosity
0     # Long run mode
0     # Record statistical errors
```

```
0.    # Step size, if ==0.0 boundary crossing mode used
5     # Runtime efficiency calculation; (0,1,2,4,5, or 6)
$type # Source type (1=isotropic, 2=Cerenkov 5=EM shower)
0     # Extended source (0) no (1) yes
1.    # Shower energy (for extended shower sources) (GeV)
-1    # Radius of volume source (m)
$ang  # Source axis angle (deg)
0     # Radial source offset wrt active volume center (m)
0     # Vertical source offset wrt active volume center (m)
2     # Geometry type (1=spherical, 2=cylindrical, 3=cubic)
30    # Bins dimension 1  (Radial or X dimension)
0     #   Lower recordable limit of dimension 1 (m)
580   #   Upper recordable limit of dimension 1 (m)
0     #   Lower active limit of dimension 1 (m)
680   #   Upper active limit of dimension 1 (m)
9     # Bins dimension 2 (Azimuthal angle wrt emission axis)
0     #   Lower recordable limit for dimension 2 (deg)
180   #   Upper recordable limit for dimension 2 (deg)
0     #   Lower active limit for dimension 2 (deg)
180   #   Upper active limit for dimension 2 (deg)
65    # Bins dimension 3,  (Zenith or Z dimension)
-580  #   Lower recordable limit of dimension 3 (deg or m)
580   #   Upper recordable limit of dimension 3 (deg or m)
-680  #   Lower active limit of dimension 3 (deg or m)
680   #   Upper active limit of dimension 3 (deg or m)
1     # Bins, emission zenith angle
0     #   Lower recordable limit for emission angle (deg)
180   #   Upper recordable limit for emission angle (deg)
0     #   Lower active limit for emission angle (deg)
180   #   Upper active limit for emission angle (deg)
1     # Bins, arrival zenith angle
0     #   Lower recordable limit for arrival angle (deg)
180   #   Upper recordable limit for arrival angle (deg)
0     #   Lower active limit for arrival angle (deg)
180   #   Upper active limit for arrival angle (deg)
50    # Timing bins
```

```
0     #   Lower recordable limit for time delay (ns)
7000  #   Upper recordable limit for time delay (ns)
0     #   Lower active limit for time delay (ns)
7000  #   Upper active limit for time delay (ns)
$depth     # Active volume vertical offset wrt ice origin
2     # Distance scaling (1=liner, 2=quadratic)
2     # Time scaling (1=linear, 2=quadratic)
-1    # (Photon wavelength (nm) or (-1) for Cerenkov light
$nph  # Number of photons to propagate
$ICE  # Ice properties input file
$EFF  # File with efficiency table selections
$TMP_PT # MC output file name
-1 # ref n_g (you must use defaults, specified by: -1)
-1 # ref n_p (you must use defaults, specified by: -1)
-1 # Importance sampling factor for scat length scaling(-1 = off)
-1 # Importance sampling factor for HG tau scaling(-1 = off)
-1 # Fraction of <cos>=0 scatters (for water) -1 == off.
```

Muon Configuration

Level 2 tables have a slightly differing geometry, as described below.

```
var_L='600'; # Active cylinder length
var_b='200'; # Position of muon vertex wrt cylinder start
var_l='60';  # Number of lengthwise bins (equidistant)
var_R='580'; # Active cylinder radius ##  450 investigate this
var_r='30';  # Number of radial bins  ##  30
var_q='YES'; # YES/NO: quadratic scaling for radial bins
var_a='9';   # Number of azimuthal bins in active cylinder
var_s='1';   # Stepping distance during generation of muon light
var_T='7000';# Time window length
var_t='50';  # Number of time bins
var_Q='YES'; # YES/NO Quadratic scaling for time bins
var_t0='3';  # Time ref: 1 muon origin, 2 muon POCA,
                  3 direct photon arrival
```

Efficiency File

Each Photonics table requires the input of the following efficiency file; the same efficiency file as used in the production set of AHA tables.

```
GLASS_N     0       # Glass index of refraction 1.48 all
GEL_N       0       # Gel index of refraction   1.41 all
QE          5       # PMT quantum efficiency
GLASS       0       # Glass transmittance
GEL         0       # Gel transmittance
SENS        5       # OM angular sensitivity 1. all
HOLE        2       # Hole ice model
OM_CORR     0       # OM curvature correction
DYNODE      1       # 1st dynode collection efficiency
PMT         1       # PMT collection area in m^2
```

Bibliography

[1] ANTARES homepage. *http://antares.in2p3.fr*.

[2] Baikal homepage. *http://www.ifh.de/baikal/baikalhome.html*.

[3] CORSIKA home page. *http://www-ik.fzk.de/corsika/*.

[4] KM3NeT homepage. *http://www.km3net.org*.

[5] NEMO homepage. *http://nemoweb.lns.infn.it/*.

[6] NESTOR scientific programme. *http://www.nestor.org.gr/*.

[7] M. Ackermann et al. Optical properties of deep glacial ice at the South Pole. *J. Geophys. Res., doi*, 10, 2006.

[8] Alekseev et al. Detection of the neutrino signal from sn 1987a using the inr baksan underground scintillation telescope. *IN: Neutrino physics; Proceedings of the International Workshop, Heidelberg, Federal Republic of Germany, Oct. 20-22, 1987*, pages 288–298, 1988.

[9] P. Askebjer, S. Barwick, L. Bergström, A. Bouchta, S. Carius, A. Coulthard, K. Engel, B. Erlandsson, A. Goobar, L. Gray, et al. Optical Properties of the South Pole Ice at Depths Between 0.8 and 1 km. *Arxiv preprint astro-ph/9412028*, 1994.

[10] Barwick Group. AMANDA-II project. *http://amanda.uci.edu/*.

[11] I. Basile, J. Petit, S. Touron, F. Grousset, and N. Barkov. Volcanic layers in Antarctic (Vostok) ice cores: Source identification and atmospheric implications. *Journal of Geophysical Research*, 106(D23):31915–31932, 2001.

[12] R. Bay, N. Bramall, and P. Price. Bipolar correlation of volcanism with millennial climate change. *Proceedings of the National Academy of Sciences*, 101(17):6341–6345, 2004.

[13] R. Bay, N. Bramall, P. Price, G. Clow, R. Hawley, R. Udisti, and E. Castellano. Globally synchronous ice core volcanic tracers and abrupt cooling during the last glacial period. *Journal of Geophysical Research*, 111(D11), 2006.

[14] R. C. Bay. Private communication.

[15] R. Bionta, G. Blewitt, C. Bratton, D. Casper, A. Ciocio, R. Claus, B. Cortez, M. Crouch, S. Dye, S. Errede, et al. Observation of a neutrino burst in coincidence with supernova 1987A in the Large Magellanic Cloud. *Physical Review Letters*, 58(14):1494–1496, 1987.

[16] N. Bramall, R. Bay, K. Woschnagg, R. Rohde, and P. Price. A deep high-resolution optical log of dust, ash, and stratigraphy in South Pole glacial ice. *Geophysical Research Letters*, 32(21), 2005.

[17] R. Brun and F. Rademakers. ROOT - an object oriented data analysis framework. In *Proceedings AIHENP'96 Workshop, Lausanne, Sep. 1996, Nucl. Inst. & Meth. in Phys. Res. A 389 (1997) 81-86. See also http://root.cern.ch/.*

[18] T. Burgess. PSI online documentation. *http://www.physto.se/~burgess/icecube /PSInterface/Doxygen/.*

[19] P. Cerenkov. Visible radiation produced by electrons moving in a medium with velocities exceeding that of light. *Phys. Rev*, 52:378–379, 1937.

[20] J. Dumm. Comparing data, aha simulation and millenium simulation. *http://icecube.wisc.edu/~jdumm/ice_comparisons/.*

[21] Y. He and P. Price. Remote sensing of dust in deep ice at the South Pole. *Journal of Geophysical Research*, 103(D14):17041–17056, 1998.

[22] S. Hickford. Simulation of cascades for icecube neutrino telescope. Master's thesis, Department of Physics and Astronomy, University of Canterbury, 2007.

[23] K. Hirata, T. Kajita, M. Koshiba, M. Nakahata, Y. Oyama, N. Sato, A. Suzuki, M. Takita, Y. Totsuka, T. Kifune, et al. Observation of a neutrino burst from the supernova SN1987A. *Physical Review Letters*, 58(14):1490–1493, 1987.

[24] IceCube Collaboration. IceCube homepage. *http://icecube.wisc.edu/.*

[25] IceCube Collaboration. Icecube internal wiki pages. *http://wiki.icecube.wisc.edu/index.php.*

[26] IceCube Collaboration. IceCube preliminary design document. edition 1.24, October 2001.

[27] M. Kowalski. *On the Reconstruction of Cascade-Like Events in the AMANDA Detector*. PhD thesis, Diploma thesis, Humboldt-Universitat zu Berlin, Berlin, Germany, 1999.

[28] J. Learned. DUMAND. *http://www.phys.hawaii.edu/˜dumand/*.

[29] J. Lundberg. Photonics homepage. *http://photonics.tsl.uu.se*.

[30] J. Lundberg, P. Miocinovic, T. Burgess, J. Adams, S. Hundertmark, P. Desiati, K. Woschnagg, and P. Niessen. Light tracking for glaciers and oceans–Scattering and absorption in heterogeneous media with Photonics.

[31] K. Mandli. Photonics bin optimisation. *Wuppertal AMANDA collaboration meeting - powerpoint*.

[32] G. Mie. Beiträge zur Optik trüber Medien, speziell kolloidaler Metallösungen. *Annalen der Physik*, 330(3):377–445, 1908.

[33] P. Miocinovic. *Muon energy reconstruction in the Antarctic Muon And Neutrino Detector Array (AMANDA)*. PhD thesis, UNIVERSITY of CALIFORNIA, 2001.

[34] P. Miocinovic, P. Price, and R. Bay. Rapid Optical Method for Logging Dust Concentration Versus Depth in Glacial Ice. *Appl. Opt*, 40:2515–2521, 2001.

[35] A. Penzias and R. Wilson. A Measurement of Excess Antenna Temperature at 4080 Mc/s. *Astrophysical Journal*, 142:419–421, 1965.

[36] D. Perkins. *Introduction to High Energy Physics*. Cambridge University Press, 2000.

[37] P. Price and L. Bergström. Optical properties of deep ice at the South Pole: scattering. *Radio detection of high energy particles; First International Workshop: RADHEP 2000, Los Angeles, CA*, pages 139–146, 16-18 Nov. 2000.

[38] S. Razzaque, S. Seunarine, D. Besson, and D. McKay. Signal Characteristics from Electromagnetic Cascades in Ice. *Nature*, 178(4531):446–449, 1956.

[39] F. Reines and C. Cowan. The Neutrino. *Nature*, 178(4531):446–449, 1956.

[40] T. Uchida, W. Shimada, T. Hondoh, S. Mae, and N. Barkov. Refractive-index measurements of natural air-hydrate crystals in an Antarctic ice sheet. *Appl. Opt*, 34(25):5746–5749, 1995.

[41] S. Warren. Optical constants of ice from the ultraviolet to the Infrared. *APPLIED OPTICS*, 23(8/15), 1984.

Acknowledgements

Without the support and enthusiasm shown by my supervisors Dr. Jenni Adams and Dr. Suruj Seunarine this thesis would not have been possible. Since introducing me to neutrino particle physics and the IceCube project, they have been a constant source of help throughout the course of my Masters studies, and for that I thank them very much.

Thanks go to everyone who has helped me with the various aspects required to bring together this thesis, especially Johan Lundberg and Predrag Miočinović for their help with Photonics, Matthias Danninger for his help with simulation and reconstruction, Jon Dumm for his help in comparing simulation results, Ewan Orr for LaTeX help and my office mates, flatmates and fellow postgraduate physics students for being themselves. For proofreading and encouragement throughout I'd like to thank my parents. Finally, I would like to thank Hana for always being there.